

**Flavor and new physics opportunities with rare charm decays into leptons**Stefan de Boer<sup>\*</sup> and Gudrun Hiller<sup>†</sup>*Fakultät für Physik, TU Dortmund, Otto-Hahn-Straße 4, D-44221 Dortmund, Germany*

(Received 15 October 2015; published 1 April 2016)

Updated standard model predictions for  $D_{(s)} \rightarrow Pl^+l^-$ ,  $l = e, \mu$ ,  $P = \pi, K$  and inclusive decays are presented. Model-independent constraints on  $|\Delta C| = |\Delta U| = 1$  Wilson coefficients are worked out. New physics (NP) opportunities do arise in semileptonic branching ratios for very large couplings only, however, are not excluded outside the resonance regions yet. The NP potential of resonance-assisted  $CP$  asymmetries and angular observables is worked out. Predictions are given for leptoquark models and include lepton flavor-violating and dineutrino decays. Whether NP can be seen depends on flavor patterns, and vice versa.

DOI: 10.1103/PhysRevD.93.074001

**I. INTRODUCTION**

The study of flavor-changing neutral current (FCNC) transitions is a key tool to explore the generational structure of standard model (SM) fermions and to look for physics beyond the standard model (BSM). While analyses involving  $b$  quarks are matured to precision level [1], the investigation of charm FCNCs is much less advanced, as corresponding rates are highly GIM suppressed and experimentally challenging and/or decay modes subjected to resonance contributions, shielding the electroweak physics.

Semileptonic charm hadron decays provide an opportunity to probe for new physics in  $|\Delta C| = |\Delta U| = 1$  FCNCs [2]. Such processes, induced by  $c \rightarrow ul^+l^-$ ,  $l = e, \mu$ , allow us to kinematically reduce the resonance background via  $c \rightarrow Mu \rightarrow l^+l^-u$ , where  $M$  denotes a meson with mass  $m_M$  decaying to dileptons such as  $M = \eta^{(\prime)}, \rho, \omega, \phi$ , by kinematic cuts in the dilepton invariant mass squared  $q^2$ , notably  $q^2 \gtrsim m_\phi^2$ . The available phase space is, however, limited, at most  $\Delta q^2 \sim 2 \text{ GeV}^2$  for the most favorable decays  $D^+ \rightarrow \pi^+l^+l^-$ , and the resonance tails remain overwhelming in the decay rates until the endpoint. Accessing short-distance physics is still possible in two situations: (i) when BSM-induced rates are much larger than the SM background and (ii) using SM null tests, that is, specifically chosen observables. The latter are generically related to SM (approximate) symmetries, such as  $CP$  in  $c \rightarrow u$  transitions, and include various ratios and asymmetries.

In this work we pursue the analysis of rare charm observables using  $CP$  asymmetries and those related to leptons, lepton flavor-violating (LFV) decays  $c \rightarrow ue^\pm\mu^\mp$ . The latter have essentially no SM contribution due to the smallness of neutrino masses. Importantly, there are no photon-induced dilepton effects, the usual source of

resonance pollution. Therefore, for LFV charm decays, no cuts in  $q^2$  are required from the theory perspective. Similarly,  $c \rightarrow uv\bar{v}$  processes have essentially zero SM background and factorize in the full region of  $q^2$ . In addition, the study of rare charm decays has great prospects at the LHCb and Belle II experiments, as well as BES III [3], and possible other future high luminosity flavor facilities [4,5].

Leptoquarks are particularly interesting for flavor physics because they link quark flavor to lepton flavor. A rich phenomenology and correlations between different kinds of flavor transitions,  $K, D$  and  $B$  decays as well as LFV, allow us to probe the SM and flavor models simultaneously. Naturally,  $CP$  violation, lepton nonuniversality (LNU) and LFV arise. We work out correlations in a number of flavor benchmarks for scalar and vector leptoquarks that induce  $c \rightarrow ul^+l^-$ . Some of these are currently discussed in the context of  $B$ -physics anomalies hinting at LNU [6–10].

The plan of the paper is as follows: In Sec. II we work out SM predictions for  $c \rightarrow ul^+l^-$  processes, including recent results for higher order perturbative contributions [11]. We identify BSM windows in rare exclusive  $c \rightarrow ul^+l^-$  modes. In Sec. III constraints and predictions are worked out model independently and within leptoquark scenarios, amended by flavor patterns. In Sec. IV we summarize. Auxiliary information is compiled in several appendixes.

**II. STANDARD MODEL PREDICTIONS**

We work out SM predictions for exclusive semileptonic charm decays. In Sec. II A we obtain (next-to-)next-to-leading-order [(N)NLO] results for the (effective)  $|\Delta C| = |\Delta U| = 1$  coefficients. In Sec. II B we work out branching ratios, including resonance effects, and compare to data.

**A. Wilson coefficients**

We write the  $c \rightarrow ul^+l^-$  effective weak Lagrangian [11–13] with two-step matching at the  $W$ -mass scale and the  $b$ -quark mass scale, respectively, as

<sup>\*</sup>stefan.deboer@tu-dortmund.de<sup>†</sup>ghiller@physik.uni-dortmund.de

$$\mathcal{L}_{\text{eff}}^{\text{weak}}|_{m_W \geq \mu > m_b} = \frac{4G_F}{\sqrt{2}} \sum_{q=d,s,b} V_{cq}^* V_{uq} (\tilde{C}_1(\mu) P_1^{(q)}(\mu) + \tilde{C}_2(\mu) P_2^{(q)}(\mu)), \quad (1)$$

$$\mathcal{L}_{\text{eff}}^{\text{weak}}|_{m_b > \mu \geq m_c} = \frac{4G_F}{\sqrt{2}} \sum_{q=d,s} V_{cq}^* V_{uq} \left( \tilde{C}_1(\mu) P_1^{(q)}(\mu) + \tilde{C}_2(\mu) P_2^{(q)}(\mu) + \sum_{i=3}^{10} \tilde{C}_i(\mu) P_i(\mu) \right). \quad (2)$$

Here,  $G_F$  is the Fermi constant and  $V_{ij}$  denote the Cabibbo-Kobayashi-Maskawa (CKM) matrix elements. Within the OPE (1) and (2), heavy fields are integrated in the Wilson coefficients  $\tilde{C}_i$  and the operators  $P_i$  are composed out of light fields. The SM operators up to dimension six read [14–16]

$$P_1^{(q)} = (\bar{u}_L \gamma_{\mu_1} T^a q_L) (\bar{q}_L \gamma^{\mu_1} T^a c_L), \quad (3)$$

$$P_2^{(q)} = (\bar{u}_L \gamma_{\mu_1} q_L) (\bar{q}_L \gamma^{\mu_1} c_L), \quad (4)$$

$$P_3 = (\bar{u}_L \gamma_{\mu_1} c_L) \sum_{\{q: m_q < \mu\}} (\bar{q} \gamma^{\mu_1} q), \quad (5)$$

$$P_4 = (\bar{u}_L \gamma_{\mu_1} T^a c_L) \sum_{\{q: m_q < \mu\}} (\bar{q} \gamma^{\mu_1} T^a q), \quad (6)$$

$$P_5 = (\bar{u}_L \gamma_{\mu_1} \gamma_{\mu_2} \gamma_{\mu_3} c_L) \sum_{\{q: m_q < \mu\}} (\bar{q} \gamma^{\mu_1} \gamma^{\mu_2} \gamma^{\mu_3} q), \quad (7)$$

$$P_6 = (\bar{u}_L \gamma_{\mu_1} \gamma_{\mu_2} \gamma_{\mu_3} T^a c_L) \sum_{\{q: m_q < \mu\}} (\bar{q} \gamma^{\mu_1} \gamma^{\mu_2} \gamma^{\mu_3} T^a q), \quad (8)$$

$$P_7 = \frac{e}{g_s} m_c (\bar{u}_L \sigma^{\mu_1 \mu_2} c_R) F_{\mu_1 \mu_2}, \quad (9)$$

$$P_8 = \frac{1}{g_s} m_c (\bar{u}_L \sigma^{\mu_1 \mu_2} T^a c_R) G_{\mu_1 \mu_2}^a, \quad (10)$$

$$P_9 = \frac{e^2}{g_s^2} (\bar{u}_L \gamma_{\mu_1} c_L) (\bar{l} \gamma^{\mu_1} l), \quad (11)$$

$$P_{10} = \frac{e^2}{g_s^2} (\bar{u}_L \gamma_{\mu_1} c_L) (\bar{l} \gamma^{\mu_1} \gamma_5 l), \quad (12)$$

where  $q_{L,R} = (1 \mp \gamma_5)/2 q$  denotes chiral quark fields,  $T^a$  are the  $SU(3)_C$  generators,  $e$  is the electromagnetic coupling,  $g_s$  is the strong coupling,  $\sigma^{\mu_1 \mu_2} = i[\gamma^{\mu_1}, \gamma^{\mu_2}]/2$ ,  $F_{\mu_1 \mu_2}$  is the electromagnetic field strength tensor,  $G_{\mu_1 \mu_2}^a$  is the chromomagnetic field strength tensor and the covariant derivative is  $D_\mu = \partial_\mu + ig_s A_\mu^a T^a + ie Q A_\mu$ .

In this section we give results for the (N)NLO QCD SM Wilson coefficients

$$\tilde{C}_i(\mu) = \tilde{C}_i^{(0)}(\mu) + \frac{\alpha_s(\mu)}{4\pi} \tilde{C}_i^{(1)}(\mu) + \left( \frac{\alpha_s(\mu)}{4\pi} \right)^2 \tilde{C}_i^{(2)}(\mu) + \mathcal{O}(\alpha_s^3(\mu)). \quad (13)$$

$\tilde{C}_{1,2}(\mu_W)$  can be inferred from [15,17], and  $\tilde{C}_{3-10}(\mu_W) = 0$  due to CKM unitarity for vanishing light quark masses. If one were to keep finite light quark masses in the Wilson coefficients at  $\mu_W$  as in [18–20], spurious large logarithms are induced, e.g. [21],

$$\sum_{q=d,s,b} V_{cq}^* V_{uq} \tilde{C}_9^{(q)}(\mu_W) \simeq V_{cs}^* V_{us} \frac{(-2)}{9} \ln \frac{m_s^2}{m_d^2} \simeq -0.29, \quad (14)$$

a procedure that is not consistent with the factorization of scales in the effective Lagrangian [11,13]. Logarithms are resummed to all orders in perturbation theory via the renormalization group (RG) equation [17,22,23]. After RG evolution of  $\tilde{C}_{1,2}$  from  $\mu_W$  to  $\mu_b$ , we integrate out the  $b$  quark at  $\mu_b$ , which induces nonzero contributions to  $P_{3-10}$ , and then we RG evolve  $\tilde{C}_{1-10}$  from  $\mu_b$  to  $\mu_c$ . The resummation to NNLO is worked out in [11], to which we refer for details on the RG equation, anomalous dimensions and matching. The results of this NNLO evolution are included in the numerical analysis in this work. Using the parameters compiled in Appendix A, we find the SM Wilson coefficients at the charm quark mass given in Table I.

We write the matrix elements of the operators  $P_{1-6,8}$  in terms of effective Wilson coefficients  $C_{7,9}^{\text{eff}}(\mu_c)$  and  $C_{10}^{\text{eff}}(\mu_c) = 0$ . We find to one-loop order

TABLE I. The  $i$ th order contributions  $(\alpha_s/(4\pi))^i \tilde{C}_j^{(i)}$ ,  $i = 0, 1, 2$  to the SM Wilson coefficients [see Eq. (13)] at  $\mu_c = m_c$ . The last row gives their sum,  $\tilde{C}_j(m_c)$ .

	$j = 1$	$j = 2$	$j = 3$	$j = 4$	$j = 5$	$j = 6$	$j = 7$	$j = 8$	$j = 9$	$j = 10$
$\tilde{C}_j^{(0)}$	-1.0275	1.0926	-0.0036	-0.0604	0.0004	0.0007	0	0	-0.0030	0
$(\alpha_s/(4\pi)) \tilde{C}_j^{(1)}$	0.3214	-0.0549	-0.0025	-0.0312	0.0000	-0.0002	0.0035	-0.0020	-0.0064	0
$(\alpha_s/(4\pi))^2 \tilde{C}_j^{(2)}$	0.0766	-0.0037	-0.0019	-0.0008	0.0001	0.0003	0.0002	-0.0003	-0.0037	0
$\tilde{C}_j$	-0.6295	1.0340	-0.0080	-0.0924	0.0005	0.0008	0.0037	-0.0023	-0.0131	0

$$\begin{aligned}
 C_9^{\text{eff}(q)}(q^2) = & \tilde{C}_9 + \frac{\alpha_s}{4\pi} \left[ \frac{8}{27} \tilde{C}_1 + \frac{2}{9} \tilde{C}_2 - \frac{8}{9} \tilde{C}_3 - \frac{32}{27} \tilde{C}_4 - \frac{128}{9} \tilde{C}_5 - \frac{512}{27} \tilde{C}_6 \right. \\
 & + L(m_c^2, q^2) \left( \frac{28}{9} \tilde{C}_3 + \frac{16}{27} \tilde{C}_4 + \frac{304}{9} \tilde{C}_5 + \frac{256}{27} \tilde{C}_6 \right) \\
 & + L(m_s^2, q^2) \left( -\frac{4}{3} \tilde{C}_3 - \frac{40}{3} \tilde{C}_5 \right) + L(0, q^2) \left( \frac{16}{9} \tilde{C}_3 + \frac{16}{27} \tilde{C}_4 + \frac{184}{9} \tilde{C}_5 + \frac{256}{27} \tilde{C}_6 \right) \\
 & \left. + (\delta_{qs} L(m_s^2, q^2) + \delta_{qd} L(0, q^2)) \left( -\frac{8}{27} \tilde{C}_1 - \frac{2}{9} \tilde{C}_2 \right) \right] + \left( \frac{\alpha_s}{4\pi} \right)^2 F_8^{(9)}(q^2/m_c^2) C_8^{\text{eff}}, \quad (15)
 \end{aligned}$$

in agreement with the corresponding calculation in  $b$ -quark decays [24], and

$$C_7^{\text{eff}(q)}(q^2) = \tilde{C}_7 + \frac{\alpha_s}{4\pi} \sum_{i=1}^6 y_i^{(7)} \tilde{C}_i + \left( \frac{\alpha_s}{4\pi} \right)^2 \left[ \left( -\frac{1}{6} \tilde{C}_1^{(0)} + \tilde{C}_2^{(0)} \right) f(m_q^2/m_c^2) + F_8^{(7)}(q^2/m_c^2) C_8^{\text{eff}} \right] \quad (16)$$

with  $C_8^{\text{eff}} = \tilde{C}_8^{(1)} + \sum_{i=1}^6 y_i^{(8)} \tilde{C}_i^{(0)}$  and  $\tilde{C}_{1-6}$  consistently expanded to order  $\alpha_s$ . The functions  $f$ ,  $L$  and  $F_8^{(7,9)}$  and the coefficients  $y_i^{(7,8)}$  are given in Appendix B. The coefficients  $C_{7,9}^{\text{eff}} \sim V_{cb}^* V_{ub}$  induced by the two-loop matrix elements of  $P_{3-6}$  and  $C_9^{\text{eff}}$  induced by the two-loop matrix elements of  $P_{1,2}$  are not known presently and are neglected in the following analysis. Hence, the NNLO result is not known; it is labeled as (N)NLO.

For the phenomenological analyses in Secs. II B and III, it is customary to redefine the dilepton and electromagnetic dipole operators and use

$$Q_7 = \frac{m_c}{e} (\bar{u} \sigma^{\mu\nu} P_R c) F_{\mu\nu}, \quad (17)$$

$$Q_9 = (\bar{u} \gamma_\mu P_L c) (\bar{l} \gamma^\mu l), \quad (18)$$

$$Q_{10} = (\bar{u} \gamma_\mu P_L c) (\bar{l} \gamma^\mu \gamma_5 l). \quad (19)$$

Their effective coefficients  $C_{7,9,10} = C_{7,9,10}(q^2)$  are related to the ones of  $P_{7,9,10}$  as

$$\begin{aligned}
 C_{7,9,10}(\mu_c) = & \frac{4\pi}{\alpha_s(\mu_c)} [V_{cd}^* V_{ud} C_{7,9,10}^{\text{eff}(d)}(\mu_c) \\
 & + V_{cs}^* V_{us} C_{7,9,10}^{\text{eff}(s)}(\mu_c)]. \quad (20)
 \end{aligned}$$

Using  $\sum_{q=d,s,b} V_{cq}^* V_{uq} = 0$  makes manifest that the coefficients are GIM or Cabibbo suppressed, specifically,  $L(m_s^2, q^2) - L(0, q^2) = \mathcal{O}(m_s^2/m_c^2)$  at high  $q^2$ .

The effective coefficient  $C_9$ , Eq. (20), in the SM is shown in Fig. 1.  $C_7$  is not shown because its  $q^2$  dependence is negligible. Note that  $C_{10} = 0$ , and that  $C_7$  and  $C_9$  are primarily set by the matrix elements of  $P_{1,2}$ . For  $\mu_c = m_c$ ,  $C_7 \approx (-0.0011 - 0.0041i)$  and  $C_9 \approx -0.021 X_{ds}$ , where  $X_{ds} = (V_{cd}^* V_{ud} L(m_d^2, q^2) + V_{cs}^* V_{us} L(m_s^2, q^2))$ . Varying

$m_c/\sqrt{2} \leq \mu_c \leq \sqrt{2}m_c$  we find  $(-0.0014 - 0.0054i) \leq C_7 \leq (-0.00087 - 0.0033i)$  and  $-0.060 X_{ds}(\mu_c = \sqrt{2}m_c) \leq C_9 \leq 0.030 X_{ds}(\mu_c = m_c/\sqrt{2})$ . For  $q^2 \gtrsim 1 \text{ GeV}^2$ , we obtain, as a result, a small SM contribution,  $|C_9| \lesssim 5 \times 10^{-4}$ .

The one-loop contribution to  $C_9$  is suppressed by cancellations between  $\tilde{C}_1$  and  $\tilde{C}_2$ . Therefore, the two-loop matrix element of  $P_{1,2}^{(q)}(\mu_c)$ ,  $q = d, s$  inducing  $C_9$ , of the order  $|V_{cd}^* V_{ud}| \times \alpha_s(\mu_c)/(4\pi) \times \text{GIM-type } m_s^2/m_c^2$  suppression at  $q^2 = \mathcal{O}(m_c^2)$ ,<sup>1</sup> could numerically be of similar size as the (N)NLO one.

## B. Phenomenology

In this section we study the SM phenomenology of  $D^+ \rightarrow \pi^+ \mu^+ \mu^-$  decays and introduce SM null tests. Decay distributions are given in Appendix D, and the requisite form factors  $f_i$  are defined in Appendix C. In particular, in our numerical analysis the vector form factor  $f_+$  is taken from data [26], and the dipole one  $f_T$  is related to  $f_+$  through the (improved) Isgur-Wise relations at low and high  $q^2$ , between which we interpolate, cf. Appendix C. A third form factor,  $f_0$ , does not contribute at short distances as it multiplies  $C_{10}$ , which vanishes in the SM. In Fig. 5,  $f_+(q^2)$ ,  $f_T(q^2)$  and  $f_0(q^2)$ , which can contribute in SM extensions, can be seen. In our calculation we expand squared amplitudes to order  $\alpha_s^2$  and apply the pole mass for  $m_c$  in matrix elements.

Integrating the distribution in different  $q^2$  bins yields the nonresonant SM branching ratios given in Table II. The first uncertainty given corresponds to the normalization, which is dominated by the  $D$  lifetime, relative to which CKM uncertainties are subdominant. The dominant theory uncertainty stems from the charm scale  $\mu_c$ , which is varied here

<sup>1</sup>This behavior is also supported by a related calculation in  $b \rightarrow sll$  decays [25].

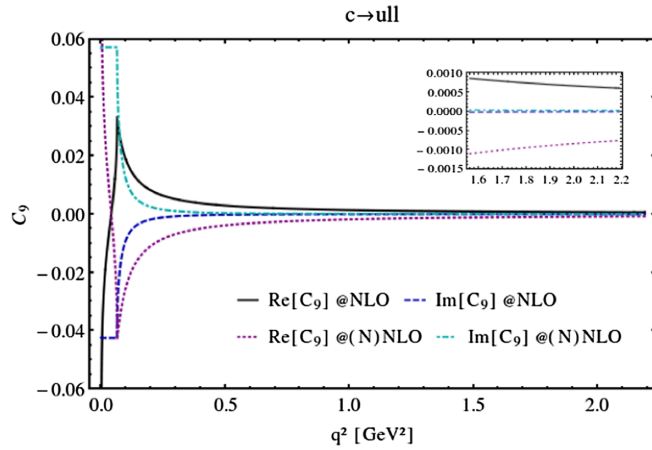


FIG. 1. The effective coefficient  $C_9(\mu_c = m_c)$  given in Eq. (20) at NLO and the pure (N)NLO terms in the SM. The two-loop matrix elements of  $P_{1,2}$  are not known presently and are not included. See text for details.

within  $m_c/\sqrt{2} \leq \mu_c \leq \sqrt{2}m_c$ . The effect of a larger upper limit on  $\mu_c$  is to enhance (decrease) the branching ratios at low (high)  $q^2$ . For instance, allowing for values of  $\mu_c$  as large as 4 GeV doubles (cuts into halves) the branching ratios obtained for  $\mu_c = \sqrt{2}m_c$  at low (high)  $q^2$ . Consequently, the effect on the full  $q^2$  range of integration averages out. The other scales are varied within  $m_{W,b}/2 \leq \mu_{W,b} \leq 2m_{W,b}$ . Uncertainties due to power corrections are not included. Electroweak corrections, which are subleading relative to QCD ones, are neglected. We checked this explicitly by calculating the effects of electromagnetic mixing among the  $P_i$  at leading order [28,29]. Additional uncertainties from  $\alpha_s(m_Z) = 0.1185 \pm 0.0006$  amount to a few percent.

Further nonresonant SM branching fractions for inclusive  $c \rightarrow ull$  decays and additional  $D \rightarrow Pll$  decays are also worked out and given in Appendix E. Our findings are consistent with [13,30], but disagree with those of [18–20] by orders of magnitude. As already discussed around Eq. (14), this goes back to the inclusion of light quark masses in [18–20] in the matching at  $\mu_W$ .

Next we model the contributions from resonances by using a (constant width) Breit-Wigner shape for  $C_9 \rightarrow C_9^R$  for vector and  $C_P \rightarrow C_P^R$  for pseudoscalar mesons,

$$C_9^R = a_\rho e^{i\delta_\rho} \left( \frac{1}{q^2 - m_\rho^2 + im_\rho \Gamma_\rho} - \frac{1}{3} \frac{1}{q^2 - m_\omega^2 + im_\omega \Gamma_\omega} \right) + \frac{a_\phi e^{i\delta_\phi}}{q^2 - m_\phi^2 + im_\phi \Gamma_\phi},$$

$$C_P^R = \frac{a_\eta e^{i\delta_\eta}}{q^2 - m_\eta^2 + im_\eta \Gamma_\eta} + \frac{a_{\eta'}}{q^2 - m_{\eta'}^2 + im_{\eta'} \Gamma_{\eta'}}, \quad (21)$$

where  $\Gamma_M$  denotes the total width of resonance  $M = \eta^{(\prime)}, \rho, \omega, \phi$  and we safely neglected the SM's  $CP$ -violating effects. Since the branching fraction of  $D^+ \rightarrow \pi^+ \omega$  decays is not measured yet, and also to reduce the number of parameters, one can use isospin to relate it to the one of the decay  $D^+ \rightarrow \pi^+ \rho$  [30]. While there are clearly corrections to this ansatz for the  $\omega$ , these are subdominant relative to the dominant contributions from the  $\rho$  due to its large width.

Approximating  $\mathcal{B}(D^+ \rightarrow \pi^+ M(\rightarrow \mu^+ \mu^-)) \simeq \mathcal{B}(D^+ \rightarrow M \pi^+) \mathcal{B}(M \rightarrow \mu^+ \mu^-)$  and taking the right-hand side from data [31] and  $\mathcal{B}(\eta' \rightarrow \mu^+ \mu^-) \sim \mathcal{O}(10^{-7})$  [31,32], we obtain

$$a_\phi = 0.24_{-0.06}^{+0.05} \text{ GeV}^2, \quad a_\rho = 0.17 \pm 0.02 \text{ GeV}^2,$$

$$a_\eta = 0.00060_{-0.00005}^{+0.00004} \text{ GeV}^2, \quad a_{\eta'} \sim 0.0007 \text{ GeV}^2. \quad (22)$$

We note that the present experimental upper limit on  $\mathcal{B}(D^+ \rightarrow \omega \pi^+)$  yields  $a_\omega \lesssim 0.04$ , somewhat below the isospin prediction,  $a_\rho/3$ .

The SM differential branching fraction of  $D^+ \rightarrow \pi^+ \mu^+ \mu^-$  decays is shown in Fig. 2. The dominant resonance contributions above the  $\phi$  peak are due to the  $\phi$  and the  $\rho$ . The relative strong phases  $\delta_{\phi,\rho,\eta}$  are varied independently within  $-\pi$  and  $\pi$ . The dominant uncertainty stems from the unknown phases; only near the resonance peaks do the uncertainties in the factors  $a_M$  become noticeable. At high  $q^2$  the resonances die out with increasing  $q^2$ , however slowly. For instance, we obtain  $|C_9^R(1.5 \text{ GeV}^2)| \lesssim 0.8$  and  $|C_9^R(2 \text{ GeV}^2)| \lesssim 0.4$ , exceeding by many orders of magnitude the SM short-distance contribution to  $Q_9$ .

We learn the following: There is room for new physics below the current search limits [27] and above the

TABLE II. Nonresonant SM branching fractions of  $D^+ \rightarrow \pi^+ \mu^+ \mu^-$  decays normalized to the total width. Non-negligible uncertainties correspond to (normalization,  $m_c, m_s, \mu_W, \mu_b, \mu_c, f_+$ ), respectively, and are given in percent. In the last column we give the corresponding experimental 90% C.L. upper limits [27].

$q^2$ bin	$\mathcal{B}(D^+ \rightarrow \pi^+ \mu^+ \mu^-)_{\text{nr}}^{\text{SM}}$	90% C.L. [27]
Full $q^2$ : $(2m_\mu)^2 \leq q^2 \leq (m_{D^+} - m_{\pi^+})^2$	$3.7 \times 10^{-12} (\pm 1, \pm 3, {}_{-15}^{+16}, \pm 1, {}_{-1}^{+3}, {}_{-1}^{+158}, {}_{-12}^{+16})$	$7.3 \times 10^{-8}$
Low $q^2$ : $0.250^2 \text{ GeV}^2 \leq q^2 \leq 0.525^2 \text{ GeV}^2$	$7.4 \times 10^{-13} (\pm 1, \pm 4, {}_{-21}^{+23}, {}_{-11}^{+10}, {}_{-1}^{+10}, {}_{-23}^{+238}, {}_{-5}^{+6})$	$2.0 \times 10^{-8}$
High $q^2$ : $q^2 \geq 1.25^2 \text{ GeV}^2$	$7.4 \times 10^{-13} (\pm 1, \pm 6, {}_{-14}^{+15}, \pm 6, {}_{-1}^{+0}, {}_{-45}^{+136}, {}_{-20}^{+27})$	$2.6 \times 10^{-8}$

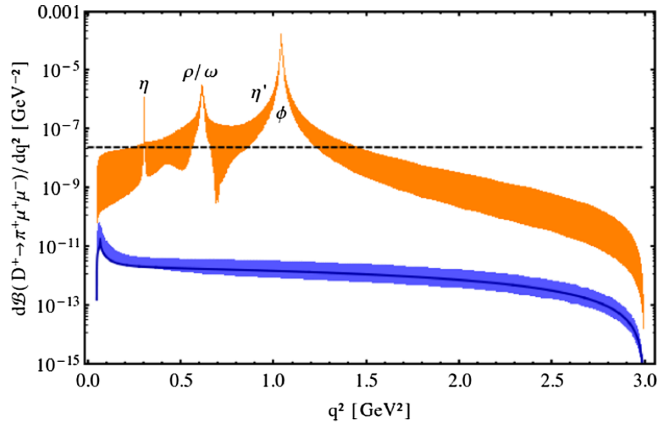


FIG. 2. The differential branching fraction  $d\mathcal{B}(D^+ \rightarrow \pi^+ \mu^+ \mu^-)/dq^2$  in the SM. The solid blue curve is the nonresonant prediction at  $\mu_c = m_c$  and the lighter blue band its  $\mu_c$  uncertainty. The orange band is the pure resonant contribution taking into account the uncertainties specified in Eq. (22) at  $1\sigma$  and varying the relative strong phases. The dashed black line denotes the 90% C.L. experimental upper limit [27].

resonance contribution; at very high and very low  $q^2$ . In either case it will require large BSM contributions to the Wilson coefficients to be above the resonant background. We will quantify this in Sec. III.

The dominance of resonances in the decay rate for SM-like Wilson coefficients is common to all  $c \rightarrow ul^+l^-$  induced processes, such as inclusive  $D \rightarrow X_u l^+ l^-$ , or other exclusive decays, e.g.,  $D \rightarrow \pi \pi l^+ l^-$  [33] and  $\Lambda_c \rightarrow p l^+ l^-$ . Choosing  $c \rightarrow ul^+l^-$  induced decay modes other than  $D^+ \rightarrow \pi^+ l^+ l^-$  does not help us gain BSM sensitivity in the dilepton spectrum; however, other modes may allow us to construct more advantageous observables. Here we discuss opportunities in semileptonic exclusive decays with observables where the resonance contribution is not obstructing SM tests.

Clean SM tests are provided by the angular distribution in  $D \rightarrow \pi l^+ l^-$  decays, notably, the lepton forward-backward asymmetry  $A_{FB}$  and the “flat” term [34],  $F_H$  (see Appendix D). Both observables are null tests of the SM and require scalar or pseudoscalar operators and tensors to be non-negligible. A promising avenue to probe operators with Lorentz structures closer to the ones present in the SM is to study  $CP$  asymmetries in the rate

$$A_{CP}(q^2) = \frac{d\Gamma/dq^2 - d\bar{\Gamma}/dq^2}{\int_{q_{\min}^2}^{q_{\max}^2} dq^2 (d\Gamma/dq^2 + d\bar{\Gamma}/dq^2)}, \quad (23)$$

where  $d\bar{\Gamma}/dq^2$  denotes the differential decay rate of the  $CP$ -conjugated mode,  $D^- \rightarrow \pi^- l^+ l^-$ . The difference of the widths can be written as

$$\begin{aligned} \frac{d\Gamma}{dq^2} - \frac{d\bar{\Gamma}}{dq^2} = & -\frac{G_F^2 \alpha_e^2}{384\pi^5 m_D^3} \sqrt{\lambda^3(m_D^2, m_P^2, q^2)} \left(1 - 4\frac{m_l^2}{q^2}\right) \\ & \times \left(1 + 2\frac{m_l^2}{q^2}\right) (\text{Im}[V_{cd}^* V_{ud}(V_{cs} V_{us}^*)] \text{Im}[c_d c_s^*] \\ & + \text{Im}[V_{cd}^* V_{ud} \Delta_9^*] \text{Im}[c_d] f_+ \\ & + \text{Im}[V_{cs}^* V_{us} \Delta_9^*] \text{Im}[c_s] f_+), \end{aligned} \quad (24)$$

where the first term in the last row corresponds to the tiny SM prediction, whereas the ones driven by  $\Delta_9 = C_9^{\text{BSM}} + C_9^C$  correspond to possible BSM contributions, and

$$c_d = \frac{4\pi}{\alpha_s} 2C_7^{\text{eff}(d)} f_T \frac{m_c}{m_D} + C_9^R|_{\rho\text{-only}} \frac{f_+}{V_{cd}^* V_{ud}}, \quad (25)$$

$$c_s = \frac{4\pi}{\alpha_s} 2C_7^{\text{eff}(s)} f_T \frac{m_c}{m_D} + C_9^R|_{\phi\text{-only}} \frac{f_+}{V_{cs}^* V_{us}}. \quad (26)$$

Here we neglect all resonances other than the  $\phi$  as the latter is dominant on the  $\phi$  and the  $\rho$ , as it is wide. To avoid double-counting we drop the perturbative contributions to  $C_9^{\text{eff}(d,s)}$  in  $c_{d,s}$ , respectively. The resonance contributions allow us to evade the otherwise strong GIM suppression, a feature already exploited in probing BSM  $CP$  violation in dipole operators on or near the  $\phi$  resonance [35]. In the SM  $CP$  violation is tiny due to the smallness of  $\text{Im}[V_{cd}^* V_{ud}(V_{cs} V_{us}^*)]$ . We find  $|A_{CP}^{\text{SM}}(q^2)| < 5 \times 10^{-3}$ , peaking at  $q^2 \sim m_\phi^2$ , where we normalized to the sum of the widths integrated over the full  $q^2$  region. We conclude that while there are large uncertainties related to the phenomenological model for  $C_9^R$ , it allows us to see large BSM effects. We show this explicitly in Sec. III, where we also study LFV decays.

### III. BEYOND THE STANDARD MODEL

We discuss testable BSM effects model independently in Sec. III A and within leptoquark models, which are introduced briefly in Secs. III B and III C.

#### A. Model-independent analysis

To study BSM effects we extend the operator basis (17)–(19),

$$\mathcal{L}_{\text{eff}}^{\text{weak}}(\mu \sim m_c) = \frac{4G_F \alpha_e}{\sqrt{2} 4\pi} \sum_i C_i^{(l)} Q_i^{(l)}, \quad (c \rightarrow ul^+l^-), \quad (27)$$

where

$$\begin{aligned}
Q_9^{(l)} &= (\bar{u}\gamma_\mu P_L c)(\bar{l}\gamma^\mu l), & Q_9^{(l)'} &= (\bar{u}\gamma_\mu P_R c)(\bar{l}\gamma^\mu l), \\
Q_{10}^{(l)} &= (\bar{u}\gamma_\mu P_L c)(\bar{l}\gamma^\mu \gamma_5 l), & Q_{10}^{(l)'} &= (\bar{u}\gamma_\mu P_R c)(\bar{l}\gamma^\mu \gamma_5 l), \\
Q_S^{(l)} &= (\bar{u}P_R c)(\bar{l}l), & Q_S^{(l)'} &= (\bar{u}P_L c)(\bar{l}l), \\
Q_P^{(l)} &= (\bar{u}P_R c)(\bar{l}\gamma_5 l), & Q_P^{(l)'} &= (\bar{u}P_L c)(\bar{l}\gamma_5 l), \\
Q_T^{(l)} &= \frac{1}{2}(\bar{u}\sigma^{\mu\nu} c)(\bar{l}\sigma_{\mu\nu} l), & Q_{T5}^{(l)} &= \frac{1}{2}(\bar{u}\sigma^{\mu\nu} c)(\bar{l}\sigma_{\mu\nu} \gamma_5 l).
\end{aligned} \tag{28}$$

$$\begin{aligned}
0.9|C_9 + C_9'|^2 + 0.9|C_{10} + C_{10}'|^2 + 4.1|C_S + C_S'|^2 + 4.2|C_P + C_P'|^2 + 1.1|C_T|^2 + 1.0|C_{T5}|^2 + 0.6\text{Re}[(C_9 + C_9')C_T^*] \\
+ 1.2\text{Re}[(C_{10} + C_{10}')(C_P + C_P')^*] + 2.3|C_7|^2 + 2.8\text{Re}[C_7(C_9 + C_9')^*] + 0.8\text{Re}[C_7C_T^*] \lesssim 1.
\end{aligned} \tag{29}$$

Analogous constraints in the full  $q^2$  region are somewhat stronger. They read

$$\begin{aligned}
1.3|C_9 + C_9'|^2 + 1.4|C_{10} + C_{10}'|^2 + 2.2|C_S + C_S'|^2 + 2.3|C_P + C_P'|^2 + 0.9|C_T|^2 + 0.8|C_{T5}|^2 + 0.9\text{Re}[(C_9 + C_9')C_T^*] \\
+ 1.0\text{Re}[(C_{10} + C_{10}')(C_P + C_P')^*] + 3.7|C_7|^2 + 4.4\text{Re}[C_7(C_9 + C_9')^*] + 1.3\text{Re}[C_7C_T^*] \lesssim 1.
\end{aligned} \tag{30}$$

The branching fraction  $\mathcal{B}(D^0 \rightarrow \mu^+\mu^-) < 6.2 \times 10^{-9}$  at CL = 90% [31] provides complementary constraints as

$$|C_S - C_S'|^2 + |C_P - C_P' + 0.1(C_{10} - C_{10}')|^2 \lesssim 0.007. \tag{31}$$

Thus,  $D \rightarrow \pi\mu\mu$  is sensitive to the complete set of operators; however, the purely leptonic decays put stronger constraints on scalar and pseudoscalar operators.

Barring cancellations, we find, consistent with [36],  $|C_{9,10}^{(l)}| \lesssim 1$ , which can exceed the resonance contribution at high  $q^2$ . Assuming no further flavor suppression for the BSM contribution  $g^2/\Lambda^2$  (weakly induced tree level) or  $g^4/(16\pi^2\Lambda^2)$  (weak loop), the limits on  $C_{9,10}^{(l)}$  imply quite mild constraints for the scale of new physics:  $\Lambda \gtrsim \mathcal{O}(5)$  TeV or  $\Lambda$  around the electroweak scale, respectively. With  $SU(2)_L$  relations  $C_9 = -C_{10}$  the bounds on new physics ease by a factor of  $1/\sqrt{2}$ . Analogous constraints on the other coefficients read  $|C_{T,T5}| \lesssim 1$  and  $|C_{S,P}^{(l)}| \lesssim 0.1$ . In Fig. 3 we illustrate BSM effects in the  $D^+ \rightarrow \pi^+\mu^+\mu^-$  differential branching fraction at high  $q^2$  with two viable choices for BSM-induced Wilson coefficients. As anticipated, the BSM distributions can exceed the SM one.

Constraints on  $c \rightarrow uee$  modes are weaker than the  $c \rightarrow u\mu\mu$  ones,  $\mathcal{B}(D^+ \rightarrow \pi^+e^+e^-) < 1.1 \times 10^{-6}$  and  $\mathcal{B}(D^0 \rightarrow e^+e^-) < 7.9 \times 10^{-8}$  at CL = 90% [31], and imply

$$\begin{aligned}
|C_{S,P}^{(e)} - C_{S,P}^{(e)'}| &\lesssim 0.3, \\
|C_{9,10}^{(e)} - C_{9,10}^{(e)'}| &\lesssim 4, \\
|C_{T,T5}^{(e)}| &\lesssim 5, & |C_7(C_9^{(e)} - C_9^{(e)'})| &\lesssim 2.
\end{aligned} \tag{32}$$

To discuss LFV we introduce the following effective Lagrangian:

As we use muonic modes frequently, in the following Wilson coefficients and operators without a lepton flavor index are understood as muonic ones, that is,  $C_i^{(\mu)} = C_i$ , etc.

Neglecting the SM Wilson coefficients, we find the following constraints on the BSM Wilson coefficients from the limits on the branching fraction of  $D^+ \rightarrow \pi^+\mu^+\mu^-$  given in Table II in the high  $q^2$  region ( $\sqrt{q^2} \geq 1.25$  GeV) at CL = 90%,

$$\begin{aligned}
\mathcal{L}_{\text{eff}}^{\text{weak}}(\mu \sim m_c) &= \frac{4G_F \alpha_e}{\sqrt{2} 4\pi} \sum_i (K_i^{(e)} O_i^{(e)} + K_i^{(\mu)} O_i^{(\mu)}), \\
(c \rightarrow ue^\pm\mu^\mp), &
\end{aligned} \tag{33}$$

where the  $K_i^{(l)}$  denote Wilson coefficients and the operators  $O_i^{(l)}$  read

$$O_9^{(e)} = (\bar{u}\gamma_\mu P_L c)(\bar{e}\gamma^\mu \mu), \quad O_9^{(\mu)} = (\bar{u}\gamma_\mu P_L c)(\bar{\mu}\gamma^\mu e), \tag{34}$$

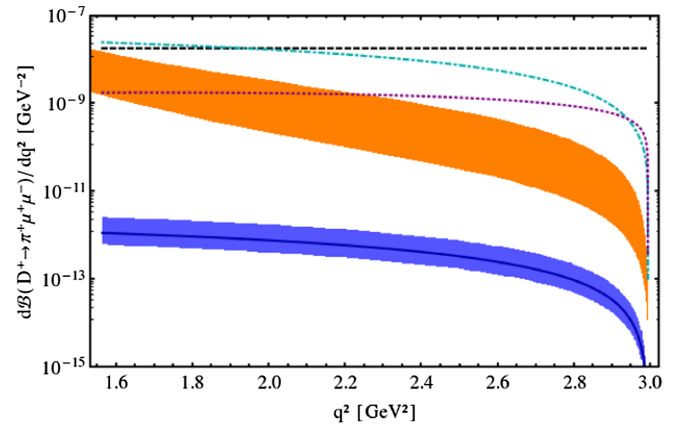


FIG. 3. The differential branching fraction  $d\mathcal{B}(D^+ \rightarrow \pi^+\mu^+\mu^-)/dq^2$  at high  $q^2$ . The solid blue curve is the nonresonant SM prediction at  $\mu_c = m_c$  and the lighter blue band its  $\mu_c$  uncertainty; the dashed black line denotes the 90% C.L. experimental upper limit [27], and the orange band shows the resonant contributions. The additional curves illustrate two viable, sample BSM scenarios,  $|C_9| = |C_{10}| = 0.6$  (dot-dashed cyan curve) and  $|C_i^{(l)}| = 0.04$  (dotted purple curve). In the latter case all BSM coefficients have been set simultaneously to this value.

with all others in analogous notation to Eq. (28). The LFV Wilson coefficients are constrained by  $\mathcal{B}(D^0 \rightarrow e^+\mu^- + e^-\mu^+) < 2.6 \times 10^{-7}$ ,  $\mathcal{B}(D^+ \rightarrow \pi^+e^+\mu^-) < 2.9 \times 10^{-6}$  and  $\mathcal{B}(D^+ \rightarrow \pi^+e^-\mu^+) < 3.6 \times 10^{-6}$  at CL = 90% [31] as

$$\begin{aligned} |K_{S,P}^{(l)} - K_{S,P}^{(l)'}| &\lesssim 0.4, \\ |K_{9,10}^{(l)} - K_{9,10}^{(l)'}| &\lesssim 6, \\ |K_{T,75}^{(l)}| &\lesssim 7, \quad l = e, \mu. \end{aligned} \quad (35)$$

The observables in the  $D \rightarrow Pl^+l^-$  angular distribution,  $A_{\text{FB}}$  and  $F_H$ , Eqs. (D2) and (D3), can be sizable while

respecting the model-independent bounds. We find that, upon  $q^2$  integration,  $|A_{\text{FB}}(D^+ \rightarrow \pi^+\mu^+\mu^-)| \lesssim 0.6$ ,  $|A_{\text{FB}}(D^+ \rightarrow \pi^+e^+e^-)| \lesssim 0.8$ ,  $F_H(D^+ \rightarrow \pi^+\mu^+\mu^-) \lesssim 1.5$  and  $F_H(D^+ \rightarrow \pi^+e^+e^-) \lesssim 1.6$ , where  $F_H^{\text{SM}}$  is below the permille level, allowing us to signal BSM physics. Here, the resonance contributions have been taken into account in the normalization to the decay rate, and both the numerator and denominator (the decay rate) have been integrated from  $q_{\text{min}}^2 = 1.25^2 \text{ GeV}^2$  to  $q_{\text{max}}^2 = (m_{D^+} - m_{\pi^+})^2$ . As the LFV bounds (35) are even weaker than the ones on the dielectron modes, sizable contributions to LFV angular observables are allowed as well. Knowing the size of LFV in more than

TABLE III. Leptoquark-fermion interactions, quantum numbers, with hypercharge  $Y = Q_e - T_3$ , and effective  $c \rightarrow u(l')^+l^-$  vertices via Fierz identities. Here,  $\tau_a$ ,  $a = 1, 2, 3$  denote the Pauli matrices, and  $\vec{\tau} \cdot \vec{X} = \sum_a \tau_a X_a$  for  $X = S_3, V_3$ . SM  $SU(2)_L$  doublets are  $\mathbf{Q}(3, 2, 1/6)$  and  $\mathbf{L}(1, 2, -1/2)$ ,  $q, q' = u, c$ , and  $l, l' = e, \mu$ .

$\subset \mathcal{L}_{LQ}$	$(SU(3)_C, SU(2)_L, Y)$	Effective vertices
$(\lambda_{S_1L} \mathbf{Q}_L^T i\tau_2 \mathbf{L}_L + \lambda_{S_1R} q_R l_R) S_1^\dagger$	$(3, 1, -1/3)$	$-\frac{(\lambda_{S_1R}^{(q'l')})^* \lambda_{S_1R}^{(q'l)}}{2m_{S_1}^2} (\bar{q}_R \gamma_\mu q'_L) (\bar{l}_R \gamma^\mu l'_R)$ $-\frac{(\lambda_{S_1L}^{(q'l')})^* \lambda_{S_1L}^{(q'l)}}{2m_{S_1}^2} (\bar{q}_L \gamma_\mu q'_L) (\bar{l}_L \gamma^\mu l'_L)$ $-\frac{(\lambda_{S_1R}^{(q'l')})^* \lambda_{S_1L}^{(q'l)}}{2m_{S_1}^2} (\bar{q}_L q'_L) (\bar{l}_L l'_R)$ $-\frac{(\lambda_{S_1L}^{(q'l')})^* \lambda_{S_1R}^{(q'l)}}{2m_{S_1}^2} (\bar{q}_R q'_L) (\bar{l}_R l'_L)$ $-\frac{(\lambda_{S_1R}^{(q'l')})^* \lambda_{S_1L}^{(q'l)}}{8m_{S_1}^2} (\bar{q} \sigma_{\mu\nu} q') (\bar{l}_L \sigma^{\mu\nu} l'_R)$ $-\frac{(\lambda_{S_1L}^{(q'l')})^* \lambda_{S_1R}^{(q'l)}}{8m_{S_1}^2} (\bar{q} \sigma_{\mu\nu} q') (\bar{l}_R \sigma^{\mu\nu} l'_L)$
$(\lambda_{S_2L} \bar{q}_R \mathbf{L}_L + \lambda_{S_2R} \bar{\mathbf{Q}}_L i\tau_2 l_R) S_2^\dagger$	$(3, 2, -7/6)$	$-\frac{\lambda_{S_2R}^{(q'l')} (\lambda_{S_2R}^{(q'l)})^*}{2m_{S_2}^2} (\bar{q}_L \gamma_\mu q'_L) (\bar{l}_R \gamma^\mu l'_R)$ $-\frac{\lambda_{S_2L}^{(q'l')} (\lambda_{S_2L}^{(q'l)})^*}{2m_{S_2}^2} (\bar{q}_R \gamma_\mu q'_R) (\bar{l}_L \gamma^\mu l'_L)$ $-\frac{\lambda_{S_2R}^{(q'l')} (\lambda_{S_2L}^{(q'l)})^*}{2m_{S_2}^2} (\bar{q}_L q'_R) (\bar{l}_L l'_R)$ $-\frac{\lambda_{S_2L}^{(q'l')} (\lambda_{S_2R}^{(q'l)})^*}{2m_{S_2}^2} (\bar{q}_R q'_L) (\bar{l}_R l'_L)$ $-\frac{\lambda_{S_2R}^{(q'l')} (\lambda_{S_2L}^{(q'l)})^*}{8m_{S_2}^2} (\bar{q} \sigma_{\mu\nu} q') (\bar{l}_L \sigma^{\mu\nu} l'_R)$ $-\frac{\lambda_{S_2L}^{(q'l')} (\lambda_{S_2R}^{(q'l)})^*}{8m_{S_2}^2} (\bar{q} \sigma_{\mu\nu} q') (\bar{l}_R \sigma^{\mu\nu} l'_L)$
$(\lambda_{S_3} \mathbf{Q}_L^T i\tau_2 \vec{\tau} \mathbf{L}_L) \cdot \vec{S}_3^\dagger$	$(3, 3, -1/3)$	$-\frac{(\lambda_{S_3}^{(q'l')})^* \lambda_{S_3}^{(q'l)}}{2m_{S_3}^2} (\bar{q}_L \gamma_\mu q'_L) (\bar{l}_L \gamma^\mu l'_L)$
$\lambda_{\tilde{V}_1} \bar{q}_R \gamma_\mu l_R (\tilde{V}_1^\mu)^\dagger$	$(3, 1, -5/3)$	$\frac{\lambda_{\tilde{V}_1}^{(q'l')} (\lambda_{\tilde{V}_1}^{(q'l)})^*}{m_{\tilde{V}_1}^2} (\bar{q}_R \gamma_\mu q'_R) (\bar{l}_R \gamma^\mu l'_R)$
$\lambda_{V_2} \mathbf{Q}_L \gamma_\mu l_R (V_2^\mu)^\dagger$	$(3, 2, -5/6)$	$\frac{(\lambda_{V_2}^{(q'l')})^* \lambda_{V_2}^{(q'l)}}{m_{V_2}^2} (\bar{q}_L \gamma_\mu q'_L) (\bar{l}_R \gamma^\mu l'_R)$
$\lambda_{\tilde{V}_2} q_R \gamma_\mu \mathbf{L}_L (\tilde{V}_2^\mu)^\dagger$	$(3, 2, 1/6)$	$\frac{(\lambda_{\tilde{V}_2}^{(q'l')})^* \lambda_{\tilde{V}_2}^{(q'l)}}{m_{\tilde{V}_2}^2} (\bar{q}_R \gamma_\mu q'_R) (\bar{l}_L \gamma^\mu l'_L)$
$\lambda_{V_3} \bar{\mathbf{Q}}_L \gamma_\mu \vec{\tau} \mathbf{L}_L \cdot (\vec{V}_3^\mu)^\dagger$	$(3, 3, -2/3)$	$\frac{2\lambda_{V_3}^{(q'l')} (\lambda_{V_3}^{(q'l)})^*}{m_{V_3}^2} (\bar{q}_L \gamma_\mu q'_L) (\bar{l}_L \gamma^\mu l'_L)$

one observable would allow us to pin down the operator structure and provide clues about the underlying model.

### B. $c \rightarrow ull$ generating models

Several models generating  $c \rightarrow ull$  transitions were studied: for instance, little Higgs models [19,30], minimal supersymmetric standard models [18,20,37,38], two Higgs doublet models [37], an up vectorlike quark singlet [38], and models with warped extra dimensions [39,40]. In all models except for the supersymmetric ones, the  $D \rightarrow \pi l^+ l^-$  branching fraction is found to be less than the resonance contributions. In the supersymmetric models the branching ratio can be close to the experimental limits. Nonvanishing asymmetries that could be  $A_{\text{FB}}$ ,  $A_{\text{CP}}$  and the  $CP$  asymmetry of  $A_{\text{FB}}$  are generically induced in BSM models [18–20,30,39,40].

Here we study effects of leptoquarks generating  $c \rightarrow ull$  transitions in a bottom-up approach. We note that in grand unified theories further model building for some representations is required [41]. For renormalizable up-type scalar and vector  $SU(2)_L$  singlet, doublet and triplet leptoquarks within the SM ( $SU(3)_C$ ,  $SU(2)_L$ ,  $U(1)_Y$ ) gauge group [42], we find, after Fierzing, the effective contributions shown in Table III. Baryon number and lepton number are conserved in the interactions. Note that models  $S_1$  and  $S_2$  contain two couplings each. Leptoquark effects in  $S_1$  have been discussed in [43].

We uniformly denote by  $M$  the mass of the leptoquarks but note that they differ, in general, depending on the representation. We assume degenerate  $SU(2)_L$ -plet masses to comply with the constraints from oblique parameters [44]. Our effective vertices agree with and extend those in [45] by considering tensor operators and relative signs. The Wilson coefficients induced by tree-level leptoquark exchanges read as

$$\begin{aligned}
 C_{9,10} &= \frac{\sqrt{2}\pi}{G_F \alpha_e} k_{9,10} \frac{\lambda_i^I (\lambda_j^I)^*}{M^2}, \\
 C'_{9,10} &= \frac{\sqrt{2}\pi}{G_F \alpha_e} k'_{9,10} \frac{\lambda_j^I (\lambda_i^I)^*}{M^2}, \\
 C_S &= C_P = \frac{\sqrt{2}\pi}{G_F \alpha_e} k_{S,P} \frac{\lambda_i^I (\lambda_j^I)^*}{M^2}, \\
 C'_S &= -C'_P = \frac{\sqrt{2}\pi}{G_F \alpha_e} k'_{S,P} \frac{\lambda_j^I (\lambda_i^I)^*}{M^2}, \\
 C_T &= \frac{\sqrt{2}\pi}{G_F \alpha_e} k_T \left( \frac{\lambda_i^I (\lambda_j^I)^*}{M^2} + \frac{\lambda_j^I (\lambda_i^I)^*}{M^2} \right), \\
 C_{T5} &= \frac{\sqrt{2}\pi}{G_F \alpha_e} k_{T5} \left( \frac{\lambda_i^I (\lambda_j^I)^*}{M^2} - \frac{\lambda_j^I (\lambda_i^I)^*}{M^2} \right), \quad (36)
 \end{aligned}$$

where  $i, j = L, R$ ; such indices are nontrivial for scenarios  $S_1$  and  $S_2$  only, which have two different couplings  $\lambda_{L,R}$  each. The correct values of  $i, j$  can also be read off from Table III. The coefficients  $k_x$  are given in Table IV.

TABLE IV. Coefficient matrix for the leptoquark Wilson coefficients (36) inducing  $c \rightarrow ull$ .

	$I$	$J$	$i$	$j$	$k_9$	$k_{10}$	$k'_9$	$k'_{10}$	$k_{S,P}$	$k'_{S,P}$	$k_T$	$k_{T5}$
$S_1$	( $cl$ )	( $ul$ )	$L$	$R$	$-\frac{1}{4}$	$\frac{1}{4}$	$-\frac{1}{4}$	$-\frac{1}{4}$	$-\frac{1}{4}$	$-\frac{1}{4}$	$-\frac{1}{8}$	$-\frac{1}{8}$
$S_2$	( $ul$ )	( $cl$ )	$R$	$L$	$-\frac{1}{4}$	$-\frac{1}{4}$	$-\frac{1}{4}$	$\frac{1}{4}$	$-\frac{1}{4}$	$-\frac{1}{4}$	$-\frac{1}{8}$	$-\frac{1}{8}$
$S_3$	( $cl$ )	( $ul$ )	$L$		$-\frac{1}{4}$	$\frac{1}{4}$	0	0	0	0	0	0
$\tilde{V}_1$	( $ul$ )	( $cl$ )		$R$	0	0	$\frac{1}{2}$	$\frac{1}{2}$	0	0	0	0
$V_2$	( $cl$ )	( $ul$ )	$R$		$\frac{1}{2}$	$\frac{1}{2}$	0	0	0	0	0	0
$\tilde{V}_2$	( $cl$ )	( $ul$ )		$L$	0	0	$\frac{1}{2}$	$-\frac{1}{2}$	0	0	0	0
$V_3$	( $ul$ )	( $cl$ )	$L$		1	-1	0	0	0	0	0	0

### C. Leptoquark phenomenology

Experimental constraints on leptoquark couplings are worked out in Appendix F. While generically  $|\lambda^{(q)}| \lesssim \mathcal{O}(0.1) [M/\text{TeV}]$  for any coupling to the first two generations and for any scenario of Table III, several flavor combinations are more severely constrained. In addition, bounds for specific models making use of correlations can be much stronger.

The  $|\Delta C| = |\Delta U| = 1$  couplings in leptoquark scenarios involving doublet quarks  $\mathbf{Q}$  are subject to constraints from the kaon sector (Table XV). Corresponding limits on the Wilson coefficients for  $c \rightarrow ull^{(\prime)}$  are given in Table V. Only the scenarios  $\tilde{V}_1$  and  $\tilde{V}_2$ , as well as the  $S_1|_R$  and  $S_2|_L$  couplings, do not receive such constraints. Hence, allow, in general, for larger effects for  $c \rightarrow ull$ ; however, decouple without further input from the  $K$  and  $B$  sectors.

Products of two Wilson coefficients are constrained by the strong limits on  $\mu - e$  conversion and  $\mu \rightarrow e\gamma$  (see Table VI). Future experiments on  $\mu \rightarrow e\gamma$  [46] and  $\mu - e$  conversion [47,48] can improve the limits by at least 2 orders of magnitude.

Further bounds and correlations depend on the flavor structure. To make progress here we study benchmark patterns of leptoquark coupling matrices  $\lambda$  put forward in [49] for quark-L-type Yukawa couplings based on flavor symmetries. Rows label quark flavors, and columns label lepton flavors. The use of discrete non-Abelian symmetries for the leptons, specifically  $A_4$  [50,51], results in textures

TABLE V. Upper limits on the  $c \rightarrow ull^{(\prime)}$  Wilson coefficients  $|C_{9,10}^{(\prime)}|$  abbreviated as  $(ll^{(\prime)})$  in leptoquark scenarios from kaon decays. For  $S_{1,2}$  the limits apply to the indicated handedness of couplings only.

	( $ee$ )	( $e\mu$ ), ( $\mu e$ )	( $\mu\mu$ )
$S_1 _L$	$\lesssim 4 \times 10^{-3}$	$\lesssim 4 \times 10^{-3}$	$\lesssim 4 \times 10^{-3}$
$S_2 _R, V_2$	$\lesssim 3 \times 10^{-2}$	$\lesssim 2 \times 10^{-4}$	$\lesssim 4 \times 10^{-3}$
$S_3, V_3$	$\lesssim 4 \times 10^{-3}$	$\lesssim 2 \times 10^{-4}$	$\lesssim 4 \times 10^{-3}$

TABLE VI. Upper limits on the products of two  $c \rightarrow ull^{(\prime)}$  Wilson coefficients  $|C_i^{(e)(\prime)} C_i^{(\mu)(\prime)}|$ , “ $(ee)(\mu\mu)$ ”, and  $|K_i^{(e)(\prime)} K_i^{(\mu)(\prime)}|$ , “ $(e\mu)(\mu e)$ ”, from  $\mu - e$  conversion and  $\mu \rightarrow e\gamma$ . The LR-mixing constraints in scenarios  $S_{1,2}$  are stronger than the unmixed ones and are given in the last row.

	$(ee)(\mu\mu), (e\mu)(\mu e)$
$S_1$	$\lesssim 2 \times 10^{-7}$
$S_2$	$\lesssim 8 \times 10^{-8}$
$S_3, \tilde{V}_1, V_2, \tilde{V}_2, V_3$	$\lesssim 6 \times 10^{-8}$
$S_{1 LR}, S_{2 LR}$	$\lesssim 2 \times 10^{-10}$

with “ones” and “zeros,” very different from the hierarchical ones in Froggatt-Nielsen  $U(1)$  models [52]. In this work we are mainly concerned with the first two generations, so our terminology reflects features of the upper-left two-by-two submatrix of  $\lambda$ . With the exception of  $D^0 \rightarrow \tau e$  and  $c \rightarrow u\bar{v}$ , the third ( $\tau, \nu_\tau$ ) column is irrelevant to our study. Similar statements hold for the third ( $t, b$ ) row, which is relevant to  $B$  physics and is linked to charm physics via flavor. We define the following:

- (i) a hierarchical flavor pattern with suppression factors for electrons,  $\kappa$ , and first and second generation quarks,  $\rho_d$  and  $\rho$ , respectively,

$$\lambda_i \sim \begin{pmatrix} \rho_d \kappa & \rho_d & \rho_d \\ \rho \kappa & \rho & \rho \\ \kappa & 1 & 1 \end{pmatrix}, \quad (37)$$

- (ii) a single lepton pattern with negligible electron couplings,

$$\lambda_{ii} \sim \begin{pmatrix} 0 & * & 0 \\ 0 & * & 0 \\ 0 & * & 0 \end{pmatrix}, \quad (38)$$

- (iii) a (first two) generation-diagonal “skewed” pattern; that is,  $\lambda^{(u\mu)}$  and  $\lambda^{(ce)}$  are negligible,

$$\lambda_{iii} \sim \begin{pmatrix} * & 0 & 0 \\ 0 & * & 0 \\ 0 & * & 0 \end{pmatrix}. \quad (39)$$

Patterns (i) and (ii) have been explicitly obtained in models where quarks are  $A_4$  singlets and hence apply to all  $u_R, d_R$  and  $\mathbf{Q}$  fields coupling to lepton doublets.<sup>2</sup> Extension of [49] to include lepton singlets as well as the skewed patterns (iii) and (iv), the latter

defined in Eq. (41), is not as straightforward and requires further model building, which is beyond the scope of this work. (Note that skewed patterns have been obtained by assigning different quark generations to different  $A_4$  singlet representations [49].)

Upper limits on rare charm branching fractions for different flavor patterns are given in Table VII. Here, for patterns (ii) and (iii) we distinguish between leptoquark scenarios which can escape kaon bounds,  $S_{1,2}, \tilde{V}_{1,2}$ , (ii.1) and (iii.1), and those subject to kaon bounds,  $S_3, V_{2,3}$ , (ii.2) and (iii.2). If  $\kappa$  is small the hierarchical flavor pattern (i) effectively reduces to pattern (ii).

The  $c \rightarrow ue^+e^-$  Wilson coefficients vanish in patterns (ii) and (iii). In pattern (i) they are driven by  $\rho_d \rho \kappa^2$  and correlated with LFV; hence, they are subject to the bounds in Table VI. We find that no BSM signal can be seen in  $c \rightarrow ue^+e^-$  branching ratios.

In pattern (ii.1) the muon Wilson coefficients are constrained by  $D^+ \rightarrow \pi^+ \mu^+ \mu^-$  and  $D^0 \rightarrow \mu^+ \mu^-$  as discussed in Sec. III A. For (ii.2) the constraints on the muon Wilson coefficients are given in Table V. In the case of (iii) the  $c \rightarrow u\mu^+ \mu^-$  Wilson coefficients vanish.

The dineutrino mode is induced in  $S_{2,3}, \tilde{V}_2$  and  $V_3$  models because those contain the requisite electromagnetic charge  $+2/3e$  leptoquark. The decay  $D \rightarrow \pi\nu\bar{\nu}$  has backgrounds from  $D \rightarrow \tau(\rightarrow \pi\nu)\bar{\nu}$ , which can be controlled by kinematic cuts  $q^2 > (m_\tau^2 - m_{\pi^+}^2)(m_{D^+}^2 - m_\tau^2)/m_\tau^2 \approx 0.34 \text{ GeV}^2$  [18,53].

The LFV transition  $c \rightarrow u\mu^-e^+$  ( $c \rightarrow u\mu^+e^-$ ) is mediated by a generation-diagonally coupling leptoquark with electric charge  $5/3e$  ( $-1/3e$ ). Therefore, for case (iii), for charge  $-1/3e$ ,  $\mathcal{B}(D^0 \rightarrow \mu^-e^+)$  and  $\mathcal{B}(\bar{D}^0 \rightarrow \mu^+e^-)$  vanish, or for charge  $5/3e$ ,  $\mathcal{B}(D^0 \rightarrow \mu^+e^-)$  and  $\mathcal{B}(\bar{D}^0 \rightarrow \mu^-e^+)$  vanish. Analogous statements hold for  $D^+ \rightarrow \pi^+e^\pm\mu^\mp$  decays. For (iii.1) the LFV Wilson coefficients are  $\lesssim \mathcal{O}(1-10)$  [see Eq. (35)], and for (iii.2) the constraints on the LFV Wilson coefficients from Table V apply. For (ii) the LFV Wilson coefficients vanish.

Complex couplings are additionally constrained by electron and neutron electric dipole moments as  $\text{Im}[C_i^{(e)}] \lesssim 4 \times 10^{-9}$  and  $\text{Im}[C_i^{(\mu)}] \lesssim 4 \times 10^{-6}$ ,  $i = S, P, T, T5$ , respectively. The  $D^+ \rightarrow \pi^+ \mu^+ \mu^-$   $CP$  asymmetry in the rate, Eq. (23), is shown for the muons-only pattern (ii) in Fig. 4. Around the  $\phi$  resonance (left-handed plots),  $A_{CP}$  scales with the BSM coefficient  $\Delta_9$ , as the normalization is driven by the resonances,  $C_9^R$ , for any BSM coefficient. At high  $q^2$  (right-handed plots) the normalization depends on the value of  $\Delta_9$ . In the plot to the upper right the normalization is set by  $\Delta_9$ ; hence,  $A_{CP}$  becomes inversely proportional to  $\Delta_9$ . In the plot to the lower right, corresponding to a scenario with smaller BSM effects, (ii.2), the normalization is again dominated by the resonances. Despite the constrained Wilson coefficients the  $CP$  asymmetry can be sizable around the  $\phi$  and above in the high  $q^2$  region, in which  $|A_{CP}|$  drops towards the endpoint. If measured around the  $\phi$ , a sizable  $CP$

<sup>2</sup>We thank Ivo de Medeiros Varzielas for confirmation.

TABLE VII. Branching fractions for the full  $q^2$  region (high  $q^2$  region) for different classes of leptoquark couplings (see text). Summation of neutrino flavors is understood. ‘‘SM-like’’ denotes a branching ratio which is dominated by resonances or is of similar size as the resonance-induced one. All  $c \rightarrow ue^+e^-$  branching ratios are SM-like in the models considered. Note that in the SM  $\mathcal{B}(D^0 \rightarrow \mu\mu) \sim 10^{-13}$  [18].

	$\mathcal{B}(D^+ \rightarrow \pi^+\mu^+\mu^-)$	$\mathcal{B}(D^0 \rightarrow \mu^+\mu^-)$	$\mathcal{B}(D^+ \rightarrow \pi^+e^\pm\mu^\mp)$	$\mathcal{B}(D^0 \rightarrow \mu^\pm e^\mp)$	$\mathcal{B}(D^+ \rightarrow \pi^+\nu\bar{\nu})$
(i)	SM-like	SM-like	$\lesssim 2 \times 10^{-13}$	$\lesssim 7 \times 10^{-15}$	$\lesssim 3 \times 10^{-13}$
(ii.1)	$\lesssim 7 \times 10^{-8}$ ( $2 \times 10^{-8}$ )	$\lesssim 3 \times 10^{-9}$	0	0	$\lesssim 8 \times 10^{-8}$
(ii.2)	SM-like	$\lesssim 4 \times 10^{-13}$	0	0	$\lesssim 4 \times 10^{-12}$
(iii.1)	SM-like	SM-like	$\lesssim 2 \times 10^{-6}$	$\lesssim 4 \times 10^{-8}$	$\lesssim 2 \times 10^{-6}$
(iii.2)	SM-like	SM-like	$\lesssim 8 \times 10^{-15}$	$\lesssim 2 \times 10^{-16}$	$\lesssim 9 \times 10^{-15}$

asymmetry, while assuming different values, can arise independent of the strong phases. For the hierarchical pattern (i)  $|A_{CP}|$  is  $\lesssim 0.003$  on the  $\phi$  resonance and  $\lesssim 0.03$  at high  $q^2$ .

Interestingly, there exists an opportunity to also study  $\tau$ -lepton couplings in charm, with  $D^0 \rightarrow \tau^\pm e^\mp$  decays. The corresponding branching fractions can be inferred from Eq. (D6); the phase-space suppression relative to  $D^0 \rightarrow \mu^\pm e^\mp$  is about  $8 \times 10^{-3}$ . We find, approximately,

$$\begin{aligned} \mathcal{B}(D^0 \rightarrow \tau^\pm e^\mp) & \\ & \simeq 5 \times 10^{-9} (|1.3(K_S^{(e,\tau)} - K_S^{(e,\tau)'}) \mp (K_9^{(e,\tau)} - K_9^{(e,\tau)'})|^2 \\ & + |1.3(K_P^{(e,\tau)} - K_P^{(e,\tau)'}) + (K_{10}^{(e,\tau)} - K_{10}^{(e,\tau)'})|^2). \end{aligned} \quad (40)$$

The limits on the decays  $\tau \rightarrow e\gamma$  and  $\tau \rightarrow eee$  are not competitive with those involving muons; however,  $SU(2)$  relations imply constraints on LFV. For (axial) vector

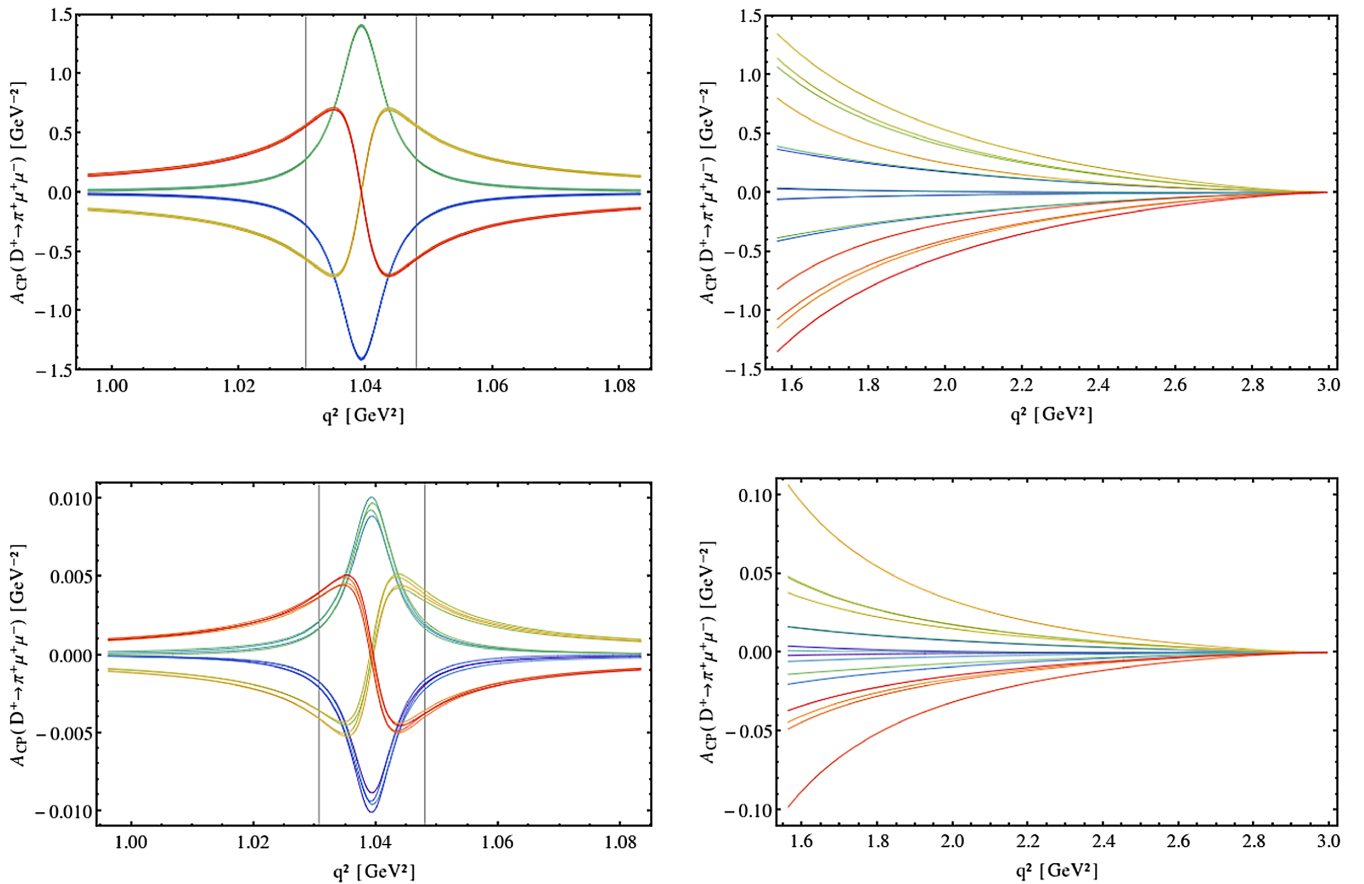


FIG. 4. The direct  $CP$  asymmetry  $A_{CP}(D^+ \rightarrow \pi^+\mu^+\mu^-)$  normalized to  $[q_{\min}^2 = (m_\phi - 5\Gamma_\phi)^2, q_{\max}^2 = (m_\phi + 5\Gamma_\phi)^2]$  (left plots) and  $[q_{\min}^2 = 1.25^2 \text{ GeV}^2, q_{\max}^2 = (m_{D^+} - m_{\pi^+})^2]$  (right plots) in case (ii.1) (upper plots) and (ii.2) (lower plots) for independent relative strong phases  $\delta_{\rho,\phi} \in \{0, \pi/2, \pi, 3\pi/2\}$ . From yellow (upper curves above  $\phi$ ) to red (lower curves above  $\phi$ ) each bunch represents  $\delta_\phi = \pi/2, \pi, 0, 3/2\pi$ .

couplings they read  $|K_{9,10}^{(e,\tau)(l)}| \lesssim 0.2$  ( $\mathcal{B}(\tau \rightarrow eK)$ ), significantly weaker than  $|K_{9,10}^{(e,\tau)}| \lesssim 4 \times 10^{-3}$  [ $\mathcal{B}(K^+ \rightarrow \pi^+ \bar{\nu}\nu)$ ], and for (pseudo)scalar Wilson coefficients  $|K_{S,P}^{(e,\tau)(l)}| \lesssim 7 \times 10^{-3}$  [ $\mathcal{B}(K^+ \rightarrow \bar{e}\nu)$ ] [54]. The hierarchical flavor pattern yields  $\mathcal{B}(D^0 \rightarrow \tau^\pm e^\mp) \lesssim 7 \times 10^{-15}$ , while the others, (ii) and (iii), give vanishing rates. One flavor pattern in which the  $SU(2)$ -related constraints are absent and which can signal LFV BSM  $D^0 \rightarrow \tau^\pm e^\mp$  decays is another skewed one, inspired by [49],

$$\lambda_{iv} \sim \begin{pmatrix} 0 & 0 & * \\ * & 0 & 0 \\ * & 0 & 0 \end{pmatrix}. \quad (41)$$

This pattern results in SM-like lepton-diagonal  $c \rightarrow ul^+l^-$ ,  $l = e, \mu$  and vanishing flavor off-diagonal  $c \rightarrow ue^\pm\mu^\mp$  modes, while  $\mathcal{B}(D \rightarrow \pi\nu\bar{\nu})$  can exceed the upper limits given in Table VII. Other flavor patterns result in a different phenomenology; hence, if measured, this allows us to learn about flavor.

#### IV. SUMMARY

Rare charm decays into leptons offer genuine avenues to search for BSM physics despite notorious resonance backgrounds. Semileptonic branching ratios  $D \rightarrow \pi l^+ l^-$  can signal BSM physics above the  $\phi$  resonance right around the current experimental limit for large BSM contributions (see Fig. 3).  $CP$  asymmetries, assisted by the resonances, observables in the angular distribution, dineutrino modes and LFV ones can signal BSM physics for much smaller BSM contributions because those correspond to SM null tests. Model-independent constraints are given in Sec. III A.

We work out correlations in several flavor benchmarks for scalar and vector leptoquark scenarios that induce  $c \rightarrow ull^{(l)}$  modes. The main results on the leptoquark phenomenology are given in Sec. III C. We find that hierarchical flavor patterns such as (37) allow only for rather limited effects in charm due to the correlations with other sectors which are subject to strong constraints. Other flavor patterns can give larger effects in branching ratios for decays into dimuons, dineutrinos and LFV ones (see Table VII). The  $CP$  asymmetry in the  $D^+ \rightarrow \pi^+ \mu^+ \mu^-$  rate provides an opportunity to probe new physics even for rather suppressed couplings in the case of leptoquarks coupling to  $SU(2)$ -doublet quarks (see the lower two plots in Fig. 4). Such asymmetries may show up, for instance, with leptoquarks  $S_3(3, 3, -1/3)$  with electron couplings sufficiently suppressed, a model that can also accommodate recent LNU hints in rare  $B \rightarrow Kl^+l^-$  decays [7,8].

The benchmark patterns studied in this work do not exhaust the flavor model space. We emphasize the importance of searches for FCNCs into dineutrinos and LFV,

including  $D^0 \rightarrow \tau^\pm e^\mp$  decays. Further experimental and theoretical study is needed to progress with the quest for BSM and flavor physics.

#### ACKNOWLEDGMENTS

We thank Christoph Bobeth, Zoltan Ligeti, Bastian Müller, and Dirk Seidel for useful comments on the manuscript. G.H. is grateful to the Kavli Institute for Theoretical Physics at Santa Barbara, where parts of this project were completed, for kind hospitality. This project is supported in part by the DFG Research Unit FOR 1873 ‘‘Quark Flavour Physics and Effective Field Theories’’ and the National Science Foundation under Grant No. NSF PHY11-25915.

*Note added.*—Recently, a related analysis [55] appeared. Note also that the recent LHCb bound  $\mathcal{B}(D^0 \rightarrow e^\pm \mu^\mp) < 1.3 \times 10^{-8}$  at 90% C.L. [56] that appeared recently starts to constrain certain leptoquark flavor scenarios (see Table VII). Furthermore, the measurement of  $\mathcal{B}(D^+ \rightarrow \omega\pi^+)$  reported in a recent preprint by BES III [57] yields  $a_\omega = 0.032_{-0.007}^{+0.006}$  GeV<sup>2</sup>, somewhat lower than the isospin prediction reported around Eq. (22).

#### APPENDIX A: PARAMETERS

$\overline{MS}$  masses are taken from [31],

$$\begin{aligned} m_t(m_t) &= 160_{-4}^{+5} \text{ GeV}, \\ m_b(m_b) &= 4.18 \pm 0.03 \text{ GeV}, \end{aligned} \quad (A1)$$

$$\begin{aligned} m_c(m_c) &= 1.275 \pm 0.025 \text{ GeV}, \\ m_s(2 \text{ GeV}) &= 0.095 \pm 0.005 \text{ GeV}. \end{aligned} \quad (A2)$$

The NNLO running, decoupling at flavor thresholds and quark pole mass are taken from [58]. The CKM matrix is given by the UTfit Collaboration [59]. The inclusive semileptonic branching fractions are given by the PDG [31], where we use  $\mathcal{B}(D \rightarrow Xl^+\nu_l) = \mathcal{B}(D \rightarrow Xl^+)$ , consistent with [60], and employ  $\mathcal{B}(D_s^+ \rightarrow X\mu^+\nu_\mu) \simeq \mathcal{B}(D_s^+ \rightarrow Xe^+\nu_e)$ . The particle masses, widths and branching fractions are given by the PDG [31]. The decay constants are given by the FLAG [61]  $f_D = 0.2092 \pm 0.0033$  GeV,  $f_{D_s^+} = 0.2486 \pm 0.0027$  GeV. The bag parameter is [62]  $B_{D^0}(\mu = 3 \text{ GeV}) = 0.757 \pm 0.028$ . We update the nuclear weak charge of cesium [63,64] using [31]  $\Delta Q_w(\text{Cs}) = 0.69 \pm 0.44$ , where  $\Delta Q_w = Q_w^{\text{exp}} - Q_w^{\text{SM}}$ .

The leptonic pion decay ratio  $R_{e/\mu}^{\text{exp}} = \Gamma(\pi^+ \rightarrow (e^+\nu_e + e^+\nu_e\gamma))/\Gamma(\pi^+ \rightarrow (\mu^+\nu_\mu + \mu^+\nu_\mu\gamma)) = (1.230 \pm 0.004) \times 10^{-4}$  [31],  $R_{e/\mu}^{\text{SM}} = (1.2352 \pm 0.0001) \times 10^{-4}$  [65] and, thus we find  $\Delta R_{e/\mu} = (-5.0 \pm 4.0) \times 10^{-7}$ . The anomalous magnetic moment of the electron is [66]  $\Delta a(e) = (-0.91 \pm 0.82) \times 10^{-12}$ . Moreover [31]

$$\Delta a(\mu) = (288 \pm 63 \pm 49) \times 10^{-11}, \quad (\text{A3})$$

$$|m_{D_1^0} - m_{D_2^0}| = (0.95_{-0.44}^{+0.41}) \times 10^{10} \text{ s}^{-1}, \quad (\text{A4})$$

$$\mathcal{B}(D^+ \rightarrow \mu^+ \nu_\mu) = (3.82 \pm 0.33) \times 10^{-4}, \quad (\text{A5})$$

$$\mathcal{B}(D_s^+ \rightarrow \mu^+ \nu_\mu) = (5.56 \pm 0.25) \times 10^{-3} \quad (\text{A6})$$

and at CL = 90% [31],

$$d(n) < 0.29 \times 10^{-25} e \text{ cm}, \quad (\text{A7})$$

$$d(e) < 10.5 \times 10^{-28} e \text{ cm}, \quad (\text{A8})$$

$$\mathcal{B}(\pi^+ \rightarrow \mu^+ \nu_e) < 8.0 \times 10^{-3}, \quad (\text{A9})$$

$$\mathcal{B}(\mu^- \rightarrow e^- \gamma) < 5.7 \times 10^{-13}, \quad (\text{A10})$$

$$\mathcal{B}(\mu^- \rightarrow e^- e^+ e^-) < 1.0 \times 10^{-12}, \quad (\text{A11})$$

$$\Gamma(\mu^- \text{Ti} \rightarrow e^- \text{Ti}) / \Gamma_{\text{capture}}(\mu^- \text{Ti}) < 4.3 \times 10^{-12}, \quad (\text{A12})$$

$$\Gamma(\mu^- \text{Au} \rightarrow e^- \text{Au}) / \Gamma_{\text{capture}}(\mu^- \text{Au}) < 7 \times 10^{-13}, \quad (\text{A13})$$

where  $\Gamma_{\text{capture}}(\mu^- \text{Ti}) = 2.59 \times 10^6 \text{ s}^{-1}$  and  $\Gamma_{\text{capture}}(\mu^- \text{Au}) = 13.07 \times 10^6 \text{ s}^{-1}$  [67].

## APPENDIX B: EFFECTIVE WILSON COEFFICIENTS

In this appendix we give auxiliary functions and coefficients of the effective Wilson coefficients defined in Sec. II A. We find

$$L(m^2, q^2) = \frac{5}{3} + \ln \frac{\mu_c^2}{m^2} + x - \frac{1}{2}(2+x)|1-x|^{1/2} \begin{cases} \ln \frac{1+\sqrt{1-x}}{1-\sqrt{1-x}} - i\pi & x \equiv \frac{(2m)^2}{q^2} < 1 \\ 2 \tan^{-1} \left[ \frac{1}{\sqrt{x-1}} \right] & x \equiv \frac{(2m)^2}{q^2} > 1, \end{cases} \quad (\text{B1})$$

and in the limit  $m^2 = 0$

$$L(0, q^2) = \frac{5}{3} + \ln \frac{\mu_c^2}{q^2} + i\pi. \quad (\text{B2})$$

We take from [12]

$$\begin{aligned} f(\rho) = & -\frac{1}{243} ((3672 - 288\pi^2 - 1296\zeta_3 + (1944 - 324\pi^2) \ln \rho + 108 \ln^2 \rho + 36 \ln^3 \rho) \rho + 576\pi^2 \rho^{\frac{3}{2}} + (324 - 576\pi^2 \\ & + (1728 - 216\pi^2) \ln \rho + 324 \ln^2 \rho + 36 \ln^3 \rho) \rho^2 + (1296 - 12\pi^2 + 1776 \ln \rho - 2052 \ln^2 \rho) \rho^3) \\ & - \frac{4\pi i}{81} ((144 - 6\pi^2 + 18 \ln \rho + 18 \ln^2 \rho) \rho + (-54 - 6\pi^2 + 108 \ln \rho + 18 \ln^2 \rho) \rho^2 + (116 - 96 \ln \rho) \rho^3) \\ & - \frac{92}{81} \ln \frac{\mu_c^2}{m_c^2} + \frac{983}{243} + \frac{52}{81} \pi i + \mathcal{O}((\rho \ln \rho)^4), \end{aligned} \quad (\text{B3})$$

where we find the constant terms from [68]. From [16] we obtain

$$y^{(7)} = \left\{ 0, 0, \frac{2}{3}, \frac{8}{9}, \frac{40}{3}, \frac{160}{9} \right\}, \quad y^{(8)} = \left\{ 0, 0, 1, -\frac{1}{6}, 20, -\frac{10}{3} \right\} \quad (\text{B4})$$

and [25]

$$\begin{aligned} F_8^{(7)}(\rho) = & \frac{8\pi^2 (2+\rho)}{27 (1-\rho)^4} - \frac{8(11-16\rho+8\rho^2)}{9 (1-\rho)^2} - \frac{16\sqrt{\rho}\sqrt{4-\rho}}{9 (1-\rho)^3} (9-5\rho+2\rho^2) \arcsin \frac{\sqrt{\rho}}{2} \\ & - \frac{32(2+\rho)}{3 (1-\rho)^4} \arcsin^2 \frac{\sqrt{\rho}}{2} - \frac{16}{9} \frac{\rho}{(1-\rho)} \ln \rho - \frac{32}{9} \ln \frac{\mu_c^2}{m_c^2} - \frac{16}{9} \pi i, \end{aligned} \quad (\text{B5})$$

$$\begin{aligned} F_8^{(9)}(\rho) = & -\frac{16\pi^2 (4-\rho)}{27 (1-\rho)^4} + \frac{16(5-2\rho)}{9 (1-\rho)^2} + \frac{32}{9} \frac{\sqrt{4-\rho}}{\sqrt{\rho}(1-\rho)^3} (4+3\rho-\rho^2) \arcsin \frac{\sqrt{\rho}}{2} \\ & + \frac{64(4-\rho)}{3 (1-\rho)^4} \arcsin^2 \frac{\sqrt{\rho}}{2} + \frac{32}{9} \frac{1}{(1-\rho)} \ln \rho. \end{aligned} \quad (\text{B6})$$

**APPENDIX C: FORM FACTORS**

We parametrize the hadronic matrix elements in terms of the form factors  $f_i(q^2)$ ,  $i = +, T, 0$ ,

$$\begin{aligned} \langle P(p_P) | \bar{u} \gamma^\mu c | D(p_D) \rangle \\ = f_+(q^2) \left( p^\mu - \frac{m_D^2 - m_P^2}{q^2} q^\mu \right) + f_0(q^2) \frac{m_D^2 - m_P^2}{q^2} q^\mu, \end{aligned} \quad (\text{C1})$$

$$\begin{aligned} \langle P(p_P) | \bar{u} \sigma^{\mu\nu} (1 \pm \gamma_5) c | D(p_D) \rangle \\ = i \frac{f_T(q^2)}{m_D} (p^\mu q^\nu - q^\mu p^\nu \pm i \epsilon^{\mu\nu\rho\sigma} p_\rho q_\sigma), \end{aligned} \quad (\text{C2})$$

where  $q^\mu = (p_D - p_P)^\mu = (p_{i^+} + p_{i^-})^\mu$  and  $p^\mu = (p_D + p_P)^\mu$ . For  $D^0 \rightarrow \pi^0$  the form factors are scaled as  $f_i \rightarrow f_i/\sqrt{2}$  by isospin. The heavy-to-light form factors are related within the heavy quark effective theory by means of a heavy quark spin symmetry [69,70]. At low recoil [71]

$$f_T(q^2) = \frac{m_D^2}{q^2} \left( 1 - \frac{\alpha_s}{\pi} \frac{1}{3} \ln \frac{\mu_c^2}{m_c^2} \right) f_+(q^2) + \mathcal{O} \left( \frac{\Lambda_{\text{QCD}}}{m_c}, \alpha_s^2 \right). \quad (\text{C3})$$

The breaking of the heavy quark spin symmetry at large recoil reads [72]

$$\begin{aligned} f_T(q^2) = \left( 1 + \frac{\alpha_s}{\pi} \left( -\frac{2}{3} \frac{2E}{m_D - 2E} \ln \frac{2E}{m_D} - \frac{1}{3} \ln \frac{\mu_c^2}{m_c^2} \right) \right) \\ \times f_+(q^2), \end{aligned} \quad (\text{C4})$$

where  $E = (m_D^2 - m_P^2 - q^2)/(2m_D)$ . In our analysis we interpolate between (C4) and (C3) and take  $f_0$  from a lattice calculation [73]. For the residual form factor we use the  $z$  expansion [26]

$$f_+(q^2) = \frac{1}{\phi(q^2, t_0)} \sum_{i=0}^{\infty} a_i(t_0) (z(q^2, t_0))^i, \quad (\text{C5})$$

with

$$\begin{aligned} z(q^2, t_0) = \frac{\sqrt{t_+ - q^2} - \sqrt{t_+ - t_0}}{\sqrt{t_+ - q^2} + \sqrt{t_+ - t_0}}, \\ t_{\pm} = (m_D \pm m_P)^2, \quad t_0 = t_+ \left( 1 - \sqrt{1 - \frac{t_-}{t_+}} \right), \end{aligned} \quad (\text{C6})$$

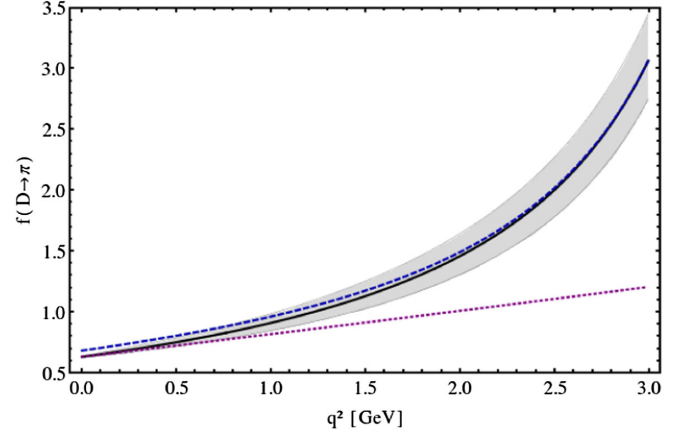


FIG. 5. The solid black line denotes  $f_+$  within its gray uncertainty band, the dashed blue curve denotes  $f_T(\mu_c = m_c)$  as derived from Eqs. (C4) and (C3), and the dotted purple curve denotes  $f_0$  as calculated on the lattice [73]. Uncertainties for  $f_T$  that follow from the parametric ones of  $f_+$  are not shown, but are included in our analysis.

$$\begin{aligned} \phi(q^2, t_0) = \sqrt{\frac{\pi m_c^2}{3}} \left( \sqrt{t_+ - q^2} + \sqrt{t_+ - t_0} \right) \\ \times \frac{t_+ - q^2}{(t_+ - t_0)^{1/4}} \frac{(\sqrt{t_+ - q^2} + \sqrt{t_+ - t_-})^{3/2}}{(\sqrt{t_+ - q^2} + \sqrt{t_+})^5}. \end{aligned} \quad (\text{C7})$$

Assuming isospin symmetry, we employ the parameters to second order as given by HFAG [26],

$$\begin{aligned} f_+(0) |V_{cd}| = 0.1425 \pm 0.0019, \quad r_1 = -1.94 \pm 0.19, \\ r_2 = -0.62 \pm 1.19, \end{aligned} \quad (\text{C8})$$

where  $r_i \equiv a_i/a_0$  and  $m_i = (m_{i^+} + m_{i^0})/2$ . Lattice computations for  $f_+(q^2)$  [73] are consistent with [26], and they find insensitivity of  $f_+$  to the spectator quark. We therefore use identical numerics for  $D \rightarrow \pi$  and  $D_s \rightarrow K$  form factors. The form factors as used in our analysis are shown in Fig. 5. We do not take into account uncertainties in  $f_0$ , which are  $\lesssim 10\%$  [73], as this enters BSM predictions only, and because they are negligible in view of other uncertainties.

**APPENDIX D: EXCLUSIVE CHARM DECAY OBSERVABLES**

Here we give the observables for exclusive charm decays used in our analysis. The form factors  $f_i$  are defined in Appendix C. We neglect nonfactorizable terms. The  $D \rightarrow P l l$  distributions are in agreement with [34]. The dilepton spectrum reads

$$\begin{aligned}
\frac{d\Gamma}{dq^2} = & \frac{G_F^2 \alpha_e^2}{1024 \pi^5 m_D^3} \left( \frac{2}{3} \left( (|C_9|^2 + |C_{10}|^2) f_+^2 + 4|C_7|^2 f_T^2 \frac{m_c^2}{m_D^2} + 4\text{Re}[C_7 C_9^*] f_T f_+ \frac{m_c}{m_D} \right) \lambda(m_D^2, m_P^2, q^2) \left( 1 + \frac{2m_l^2}{q^2} \right) \right. \\
& + |C_{10}|^2 (-f_+^2 \lambda(m_D^2, m_P^2, q^2) + f_0^2 (m_D^2 - m_P^2)^2) \frac{4m_l^2}{q^2} + (|C_S|^2 (q^2 - 4m_l^2) + |C_P|^2 q^2) f_0^2 \frac{(m_D^2 - m_P^2)^2}{m_c^2} \\
& + \frac{4}{3} (|C_T|^2 + |C_{T5}|^2) f_T^2 \frac{q^2 \lambda(m_D^2, m_P^2, q^2)}{m_D^2} \left( 1 - \frac{4m_l^2}{q^2} \right) + 8\text{Re} \left[ \left( C_9 f_+ + 2C_7 f_T \frac{m_c}{m_D} \right) C_T^* \right] f_T \frac{\lambda(m_D^2, m_P^2, q^2)}{m_D} m_l \\
& \left. + 4\text{Re}[C_{10} C_P^*] f_0^2 \frac{(m_D^2 - m_P^2)^2}{m_c} m_l + 16|C_T|^2 f_T^2 \frac{\lambda(m_D^2, m_P^2, q^2)}{m_D^2} m_l \right) \sqrt{\lambda(m_D^2, m_P^2, q^2)} \left( 1 - \frac{4m_l^2}{q^2} \right), \quad (\text{D1})
\end{aligned}$$

where  $\lambda(a, b, c) = a^2 + b^2 + c^2 - 2ab - 2ac - 2bc$ . The differential lepton forward-backward asymmetry defined as the asymmetry between forward minus backward flying  $l^-$  in the dilepton center-of-mass frame relative to the recoiling  $P$  reads

$$\begin{aligned}
A_{\text{FB}}(q^2) = & N \frac{G_F^2 \alpha_e^2}{512 \pi^5 m_D^3} \left( \text{Re}[(C_S C_T^* + C_P C_{T5}^*)] f_T \frac{m_D^2 - m_P^2}{m_c m_D} q^2 + \text{Re} \left[ \left( C_9 f_+ + 2C_7 f_T \frac{m_c}{m_D} \right) C_S^* \right] \frac{m_D^2 - m_P^2}{m_c} m_l \right. \\
& \left. + 2\text{Re}[C_{10} C_{T5}^*] f_T \frac{m_D^2 - m_P^2}{m_D} m_l \right) f_0 \lambda(m_D^2, m_P^2, q^2) \left( 1 - \frac{4m_l^2}{q^2} \right). \quad (\text{D2})
\end{aligned}$$

For vanishing lepton masses the flat term [34] reads

$$\begin{aligned}
F_H(q^2) = & N \frac{G_F^2 \alpha_e^2}{2048 \pi^5 m_D^3} \left( (|C_S|^2 + |C_P|^2) f_0^2 \frac{(m_D^2 - m_P^2)^2}{m_c^2} \right. \\
& \left. + 4(|C_T|^2 + |C_{T5}|^2) f_T^2 \frac{\lambda(m_D^2, m_P^2, q^2)}{m_D^2} \right) q^2 \sqrt{\lambda(m_D^2, m_P^2, q^2)} + \mathcal{O}(m_l), \quad (\text{D3})
\end{aligned}$$

where  $N^{-1} = \int_{q_{\text{min}}^2}^{q_{\text{max}}^2} dq^2 d\Gamma/dq^2$ . For the LFV  $D \rightarrow Pe\mu$  decay distributions we obtain, for  $m_e = 0$ ,

$$\begin{aligned}
\frac{d\Gamma(D^+ \rightarrow P^+ e^\pm \mu^\mp)}{dq^2} = & \frac{G_F^2 \alpha_e^2}{1024 \pi^5 m_D^3} \sqrt{\lambda(m_D^2, m_P^2, q^2)} \left( \frac{2}{3} (|K_9|^2 + |K_{10}|^2) f_+^2 \lambda(m_D^2, m_P^2, q^2) + (|K_S|^2 + |K_P|^2) f_0^2 \frac{(m_D^2 - m_P^2)^2}{m_c^2} q^2 \right. \\
& + \frac{4}{3} (|K_T|^2 + |K_{T5}|^2) f_T^2 \frac{q^2 \lambda(m_D^2, m_P^2, q^2)}{m_D^2} + 2\text{Re}[\pm K_9 K_S^* + K_{10} K_P^*] f_0^2 \frac{(m_D^2 - m_P^2)^2}{m_c} m_\mu \\
& \left. + 4\text{Re}[K_9 K_T^* \pm K_{10} K_{T5}^*] f_T f_+ \frac{\lambda(m_D^2, m_P^2, q^2)}{m_D} m_\mu \right) + \mathcal{O}(m_\mu^2), \quad (\text{D4})
\end{aligned}$$

where  $K_i = K_i^{(\mu)}$  and the plus signs for  $D^+ \rightarrow P^+ e^+ \mu^-$ , and  $K_i = K_i^{(e)}$  and the minus signs for  $D^+ \rightarrow P^+ e^- \mu^+$ . Compared to Eq. (D1), additional vector-scalar and axial-vector–axial-tensor terms are present in Eq. (D4).

All Wilson coefficients except for those of the tensors in Eqs. (D1)–(D4) are tacitly understood as  $C_i \rightarrow C_i + C'_i$  and  $K_i \rightarrow K_i + K'_i$ ; that is, primed Wilson coefficients are added.

The  $D^0 \rightarrow l^+ l^-$  branching fraction can be inferred from [34]

$$\mathcal{B}(D^0 \rightarrow l^+ l^-) = \frac{G_F^2 \alpha_e^2 m_{D^0}^5 f_{D^0}^2}{64 \pi^3 \Gamma_{D^0}} \sqrt{1 - \frac{4m_l^2}{m_{D^0}^2}} \left( \left( 1 - \frac{4m_l^2}{m_{D^0}^2} \right) \left| \frac{C_S - C'_S}{m_c} \right|^2 + \left| \frac{C_P - C'_P}{m_c} + \frac{2m_l}{m_{D^0}^2} (C_{10} - C'_{10}) \right|^2 \right). \quad (\text{D5})$$

The LFV ones read, for  $m_e = 0$ ,

$$\begin{aligned}
 \mathcal{B}(D^0 \rightarrow e^- \mu^+) &= \frac{G_F^2 \alpha_e^2 m_{D^0}^5 f_{D^0}^2}{64\pi^3 \Gamma_{D^0}} \left(1 - \frac{m_\mu^2}{m_{D^0}^2}\right)^2 \left( \left| \frac{K_S^{(e)} - K_S^{(e)'}}{m_c} - \frac{m_\mu}{m_{D^0}^2} (K_9^{(e)} - K_9^{(e)'}) \right|^2 \right. \\
 &\quad \left. + \left| \frac{K_P^{(e)} - K_P^{(e)'}}{m_c} + \frac{m_\mu}{m_{D^0}^2} (K_{10}^{(e)} - K_{10}^{(e)'}) \right|^2 \right), \\
 \mathcal{B}(D^0 \rightarrow \mu^- e^+) &= \frac{G_F^2 \alpha_e^2 m_{D^0}^5 f_{D^0}^2}{64\pi^3 \Gamma_{D^0}} \left(1 - \frac{m_\mu^2}{m_{D^0}^2}\right)^2 \left( \left| \frac{K_S^{(\mu)} - K_S^{(\mu)'}}{m_c} + \frac{m_\mu}{m_{D^0}^2} (K_9^{(\mu)} - K_9^{(\mu)'}) \right|^2 \right. \\
 &\quad \left. + \left| \frac{K_P^{(\mu)} - K_P^{(\mu)'}}{m_c} + \frac{m_\mu}{m_{D^0}^2} (K_{10}^{(\mu)} - K_{10}^{(\mu)'}) \right|^2 \right). \tag{D6}
 \end{aligned}$$

### APPENDIX E: NONRESONANT SM $c \rightarrow ull$ BRANCHING FRACTIONS

In this appendix we provide our predictions for the nonresonant SM branching fractions of the inclusive  $c \rightarrow ull$  decays and exclusive  $D \rightarrow Pll$  modes. In our analysis uncertainties due to power corrections are not included.

Electroweak corrections, which are subleading relative to QCD ones, are neglected. For the  $D \rightarrow Pll$  modes we integrate the branching fractions over different dilepton masses,  $\sqrt{q^2} \geq 2m_l$  (Table VIII),  $0.250 \text{ GeV} \leq \sqrt{q^2} \leq 0.525 \text{ GeV}$  (Table IX) and  $\sqrt{q^2} \geq 1.25 \text{ GeV}$  (Table X).

Next, we obtain inclusive  $c \rightarrow ull$  branching fractions. To leading order in the heavy quark expansion and neglecting lepton masses, the  $q^2$  distribution reads [74]

$$\frac{d\Gamma(c \rightarrow ull)}{dq^2} = \frac{G_F^2 \alpha_e^2 m_c^3}{768\pi^5} \left(1 - \frac{q^2}{m_c^2}\right)^2 \left[ \left(1 + 2\frac{q^2}{m_c^2}\right) (|C_9|^2 + |C_{10}|^2) + 4\left(2\frac{m_c^2}{q^2} + 1\right) |C_7|^2 + 12\text{Re}[C_7 C_9^*] \right], \tag{E1}$$

where  $q^2 = (p_c - p_u)^2 = (p_{l^+} + p_{l^-})^2$  and  $(2m_l)^2 \leq q^2 \leq m_c^2$ .

The matrix elements at NLO QCD are obtained as  $C_i \rightarrow C_i(1 + \alpha_s/\pi\sigma_i(q^2/m_c^2))$  [75] (and references therein),

$$\sigma_7(\rho) = -\frac{4}{3}\text{Li}_2[\rho] - \frac{2}{3}\ln\rho \ln[1-\rho] - \frac{2}{9}\pi^2 - \ln[1-\rho] - \frac{2}{9}(1-\rho)\ln[1-\rho] + \frac{1}{6} - \frac{4}{3}\ln\frac{\mu_c^2}{m_c^2}, \tag{E2}$$

$$\sigma_9(\rho) = -\frac{4}{3}\text{Li}_2[\rho] - \frac{2}{3}\ln\rho \ln[1-\rho] - \frac{2}{9}\pi^2 - \ln[1-\rho] - \frac{2}{9}(1-\rho)\ln[1-\rho] + \frac{3}{2}, \tag{E3}$$

where  $\sigma_{10} = \sigma_9$  and via  $\text{Re}[C_i C_j^*] \rightarrow \text{Re}[C_i C_j^*](1 + \alpha_s/\pi\tau_{ij}^{(1)}(q^2/m_c^2))$ ,

TABLE VIII. Nonresonant SM branching fractions for  $\sqrt{q^2} \geq 2m_l$  of  $D \rightarrow Pll$  decays normalized to the width. Non-negligible uncertainties are labeled by (normalization,  $m_c$ ,  $m_s$ ,  $\mu_W$ ,  $\mu_b$ ,  $\mu_c$ ,  $f_+$ ) given in percentage, where  $m_{W,b}/2 \leq \mu_{W,b} \leq 2m_{W,b}$  and  $m_c/\sqrt{2} \leq \mu_c \leq \sqrt{2}m_c$ .

Mode	Branching fraction	90% C.L. [31]
$D^+ \rightarrow \pi^+ e^+ e^-$	$4.6 \times 10^{-12} (\pm 1, {}_{-1}^{+2}, {}_{-13}^{+14}, \pm 1, {}_{-1}^{+5}, {}_{-3}^{+210}, {}_{-10}^{+13})$	$1.1 \times 10^{-6}$
$D^+ \rightarrow \pi^+ \mu^+ \mu^-$	$3.7 \times 10^{-12} (\pm 1, \pm 3, {}_{-15}^{+16}, \pm 1, {}_{-1}^{+3}, {}_{-1}^{+158}, {}_{-12}^{+16})$	$7.3 \times 10^{-8}$
$D^0 \rightarrow \pi^0 e^+ e^-$	$9.1 \times 10^{-13} (\pm 1, \pm 1, {}_{-13}^{+14}, \pm 1, {}_{-1}^{+5}, {}_{-2}^{+211}, {}_{-10}^{+13})$	$4.5 \times 10^{-5}$
$D^0 \rightarrow \pi^0 \mu^+ \mu^-$	$7.3 \times 10^{-13} (\pm 1, \pm 3, {}_{-15}^{+16}, \pm 1, {}_{-1}^{+3}, {}_{-1}^{+159}, {}_{-12}^{+16})$	$1.8 \times 10^{-4}$
$D_s^+ \rightarrow K^+ e^+ e^-$	$1.7 \times 10^{-12} (\pm 2, {}_{-3}^{+4}, {}_{-12}^{+13}, {}_{-1}^{+7}, {}_{-1}^{+8}, {}_{-7}^{+228}, {}_{-8}^{+10})$	$3.7 \times 10^{-6}$
$D_s^+ \rightarrow K^+ \mu^+ \mu^-$	$1.2 \times 10^{-12} (\pm 2, {}_{-1}^{+2}, {}_{-15}^{+16}, \pm 2, {}_{-1}^{+4}, {}_{-1}^{+167}, {}_{-10}^{+13})$	$2.1 \times 10^{-5}$

TABLE IX. As in Table VIII but for the low  $q^2$  region,  $0.250 \text{ GeV} \leq \sqrt{q^2} \leq 0.525 \text{ GeV}$ .

Mode	Branching fraction	90% C.L. [27]
$D^+ \rightarrow \pi^+ e^+ e^-$	$8.1 \times 10^{-13} (\pm 1, {}_{-4}^{+5}, {}_{-22}^{+23}, {}_{-12}^{+11}, {}_{-1}^{+10}, {}_{-24}^{+247}, \pm 5)$	
$D^+ \rightarrow \pi^+ \mu^+ \mu^-$	$7.4 \times 10^{-13} (\pm 1, \pm 4, {}_{-21}^{+23}, {}_{-11}^{+10}, {}_{-1}^{+10}, {}_{-23}^{+238}, {}_{-5}^{+6})$	$2.0 \times 10^{-8}$
$D^0 \rightarrow \pi^0 e^+ e^-$	$1.6 \times 10^{-13} (\pm 1, {}_{-4}^{+5}, {}_{-22}^{+23}, {}_{-12}^{+11}, {}_{-1}^{+10}, {}_{-24}^{+247}, \pm 5)$	
$D^0 \rightarrow \pi^0 \mu^+ \mu^-$	$1.5 \times 10^{-13} (\pm 1, \pm 4, {}_{-21}^{+23}, {}_{-11}^{+10}, {}_{-1}^{+10}, {}_{-22}^{+238}, {}_{-5}^{+6})$	
$D_s^+ \rightarrow K^+ e^+ e^-$	$3.6 \times 10^{-13} (\pm 2, \pm 5, {}_{-22}^{+23}, {}_{-13}^{+12}, {}_{-1}^{+11}, {}_{-21}^{+248}, \pm 5)$	
$D_s^+ \rightarrow K^+ \mu^+ \mu^-$	$3.3 \times 10^{-13} (\pm 2, \pm 5, {}_{-22}^{+23}, {}_{-13}^{+12}, {}_{-1}^{+11}, {}_{-20}^{+239}, {}_{-5}^{+6})$	

TABLE X. As in Table VIII but for the high  $q^2$  region,  $\sqrt{q^2} \geq 1.25 \text{ GeV}$ , and  $l = e, \mu$ .

Mode	Branching fraction	90% C.L. [27]
$D^+ \rightarrow \pi^+ l^+ l^-$	$7.4 \times 10^{-13} (\pm 1, \pm 6, {}_{-14}^{+15}, \pm 6, {}_{-14}^{+0}, {}_{-45}^{+136}, {}_{-20}^{+27})$	$2.6 \times 10^{-8} (l = \mu)$
$D^0 \rightarrow \pi^0 l^+ l^-$	$1.4 \times 10^{-13} (\pm 1, \pm 6, {}_{-14}^{+15}, \pm 6, {}_{-14}^{+0}, {}_{-45}^{+136}, {}_{-20}^{+27})$	
$D_s^+ \rightarrow K^+ l^+ l^-$	$7.9 \times 10^{-14} (\pm 2, \pm 6, {}_{-14}^{+15}, \pm 6, {}_{-14}^{+0}, {}_{-45}^{+133}, {}_{-19}^{+26})$	

$$\tau_{77}^{(1)}(\rho) = -\frac{2}{9(2+\rho)} \left( 2(1-\rho)^2 \ln[1-\rho] + \frac{6\rho(2-2\rho-\rho^2)}{(1-\rho)^2} \ln \rho + \frac{11-7\rho-10\rho^2}{1-\rho} \right), \quad (\text{E4})$$

$$\tau_{99}^{(1)}(\rho) = -\frac{4}{9(1+2\rho)} \left( 2(1-\rho)^2 \ln[1-\rho] + \frac{3\rho(1+\rho)(1-2\rho)}{(1-\rho)^2} \ln \rho + \frac{3(1-3\rho^2)}{1-\rho} \right), \quad (\text{E5})$$

$$\tau_{79}^{(1)}(\rho) = -\frac{4(1-\rho)^2}{9\rho} \ln[1-\rho] - \frac{4\rho(3-2\rho)}{9(1-\rho)^2} \ln \rho - \frac{2(5-3\rho)}{9(1-\rho)}, \quad (\text{E6})$$

$$\begin{aligned} \tau_{710}^{(1)}(\rho) = & -\frac{5}{2} + \frac{1}{3(1-3\rho)} - \frac{\rho(6-7\rho) \ln \rho}{3(1-\rho)^2} - \frac{(3-7\rho+4\rho^2) \ln[1-\rho]}{9\rho} \\ & + \frac{1}{18(1-\rho)^2} [24(1+13\rho-4\rho^2) \text{Li}_2[\sqrt{\rho}] + 12(1-17\rho+6\rho^2) \text{Li}_2[\rho] + 6\rho(6-7\rho) \ln \rho \\ & + 24(1-\rho)^2 \ln \rho \ln[1-\rho] + 12(-13+16\rho-3\rho^2)(\ln[1-\sqrt{\rho}] - \ln[1-\rho]) \\ & + 39 - 2\pi^2 + 252\rho - 26\pi^2\rho + 21\rho^2 + 8\pi^2\rho^2 - 180\sqrt{\rho} - 132\rho\sqrt{\rho}], \end{aligned} \quad (\text{E7})$$

$$\begin{aligned} \tau_{910}^{(1)}(\rho) = & -\frac{5}{2} + \frac{1}{3(1-\rho)} - \frac{\rho(6-7\rho) \ln \rho}{3(1-\rho)^2} - \frac{2(3-5\rho+2\rho^2) \ln[1-\rho]}{9\rho} \\ & - \frac{1}{18(1-\rho)^2} [48\rho(-5+2\rho) \text{Li}_2[\sqrt{\rho}] + 24(-1+7\rho-3\rho^2) \text{Li}_2[\rho] + 6\rho(-6+7\rho) \ln \rho \\ & - 24(1-\rho)^2 \ln \rho \ln[1-\rho] + 24(5-7\rho+2\rho^2)(\ln[1-\sqrt{\rho}] - \ln[1-\rho]) \\ & - 21 - 156\rho + 20\pi^2\rho + 9\rho^2 - 8\pi^2\rho^2 + 120\sqrt{\rho} + 48\rho\sqrt{\rho}], \end{aligned} \quad (\text{E8})$$

where  $\tau_{1010} = \tau_{99}$ . We obtain the NNLO term  $\delta^{(2)}|C_9|^2 = |C_9|^2(\alpha_s/\pi)^2\tau_{99}^{(2)}(q^2/m_c^2)$  as [76]

$$\begin{aligned}
 \tau_{99}^{(2)}(\rho) = & \frac{1}{(1-\rho)^2(1+2\rho)} [2(2.854 - 0.665\rho - 0.109\rho^2 - 8.572\rho^3 + 5.561\rho^4 + 0.931\rho^5) \\
 & + \frac{2}{3}(-0.063615 + 0.098146\rho + 0.144642\rho^2 - 0.307331\rho^3 + 0.107417\rho^4 + 0.020707\rho^5) \\
 & + \frac{16}{9}(3.575 - 2.867\rho + 2.241\rho^2 - 12.027\rho^3 + 11.564\rho^4 - 2.489\rho^5) \\
 & + 4(-8.151 + 2.990\rho - 3.537\rho^2 + 36.561\rho^3 - 42.275\rho^4 + 23.899\rho^5 - 9.494\rho^6)]. \quad (E9)
 \end{aligned}$$

We normalize to the  $c \rightarrow (d, s)l\nu$  width and the experimental branching fraction

$$\frac{d\mathcal{B}_{D \rightarrow X_{u\ell}l}}{dq^2} = \frac{\mathcal{B}(D \rightarrow X_{(d,s)l\nu})}{\Gamma_{c \rightarrow (d,s)l\nu}} \frac{d\Gamma_{c \rightarrow u\ell l}}{dq^2} \quad (E10)$$

with [77]

$$\Gamma_{c \rightarrow (d,s)l\nu} = \frac{G_F^2 m_c^3}{192\pi^3} \sum_{q \in \{d,s\}} |V_{cq}|^2 \left( X_0(m_q/m_c) + \frac{\alpha_s}{\pi} X_1(m_q/m_c) + \left( \frac{\alpha_s}{\pi} \right)^2 X_2(m_q/m_c) \right), \quad (E11)$$

where the functions  $X_i$  are given in [77]. Power corrections can be inferred from [78,79]. They are, however, not included in our numerical analysis, as the OPE breaks down for large  $q^2$  when the inclusive decay ceases to be inclusive but rather degenerates into a few exclusive modes. Yet, the power corrections in the region where the OPE works have a small effect on the uncertainty budget at low  $q^2$ . A comprehensive treatment of the full  $q^2$  region is beyond the scope of this work. Our resulting inclusive  $c \rightarrow ull$  branching fractions are compiled in Table XI.

## APPENDIX F: LEPTOQUARK CONSTRAINTS

In this appendix we provide constraints on the couplings of the scalar and vector leptoquarks of Table III. Collider experiments find  $M \gtrsim 1$  TeV [80,81]; thus, we use  $M = 1$  TeV as a reference. We neglect RGE effects from

TABLE XI. Nonresonant SM branching fractions for  $\sqrt{q^2} \geq 2m_l$  of  $D \rightarrow X_{u\ell}l$  decays normalized to  $D \rightarrow X_{d,s}l\nu$  and vanishing lepton masses except for the lower cut. Non-negligible uncertainties are labeled by (normalization,  $m_c$ ,  $m_s$ ,  $\mu_W$ ,  $\mu_b$ ,  $\mu_c$ ) given in percentage, where  $m_{W,b}/2 \leq \mu_{W,b} \leq 2m_{W,b}$  and  $m_c/\sqrt{2} \leq \mu_c \leq \sqrt{2}m_c$ .

Mode	Branching fraction
$D^+ \rightarrow X_u^+ e^+ e^-$	$9.4 \times 10^{-10} (\pm 2,_{-6}^{+7},_{-14}^{+16}, \pm 7, \pm 1,_{-43}^{+109})$
$D^+ \rightarrow X_u^+ \mu^+ \mu^-$	$2.0 \times 10^{-10} (\pm 19,_{-5}^{+5},_{-14}^{+15},_{-7}^{+8}, \pm 1,_{-40}^{+120})$
$D^0 \rightarrow X_u^0 e^+ e^-$	$3.8 \times 10^{-10} (\pm 2,_{-6}^{+7},_{-14}^{+16}, \pm 7, \pm 1,_{-43}^{+109})$
$D^0 \rightarrow X_u^0 \mu^+ \mu^-$	$7.7 \times 10^{-11} (\pm 9,_{-5}^{+5},_{-14}^{+15},_{-7}^{+8}, \pm 1,_{-40}^{+120})$
$D_s^+ \rightarrow X_u^+ e^+ e^-$	$3.8 \times 10^{-10} (\pm 7,_{-6}^{+7},_{-14}^{+16}, \pm 7, \pm 1,_{-43}^{+109})$
$D_s^+ \rightarrow X_u^+ \mu^+ \mu^-$	$7.5 \times 10^{-11} (\pm 7,_{-5}^{+5},_{-14}^{+15},_{-7}^{+8}, \pm 1,_{-40}^{+120})$

$M$  to  $\mu_W$ , and further to  $\mu_c$ , noting that  $Q_9$  and  $Q_{10}$  do not scale and  $C_{S,P}(\mu \sim 1 \text{ TeV}) \simeq 0.5 C_{S,P}(\mu \sim \mu_c)$  and  $C_{T,TS}(\mu \sim 1 \text{ TeV}) \simeq 1.3 C_{T,TS}(\mu \sim \mu_c)$  at one-loop QCD [34]. Neglecting such effects is within the accuracy aimed at in this work. We do not constrain non-gauge-vector leptoquarks, which could depend on the cutoff scale within some model [45]. We first list the constraints on the couplings and the related observables for scalar (Tables XII and XIII) and vector (Table XIV) leptoquarks. Our constraints are consistent with, and update and extend those of [45,54], and we note that quark doublet couplings are additionally constrained by kaon physics [45,54]. Results are given in Table XV. Next, we calculate the constraints of Tables XII–XIV, where the experimental limits are given in Appendix A. We note that fermion doublets coupling to leptoquarks are implicitly added. We obtain constraints using  $D \rightarrow Pll$  [Eq. (D1)],  $D \rightarrow Pe\mu$  [Eq. (D4)],  $D \rightarrow ll$  [Eq. (D5)] and  $D \rightarrow \mu e$  [Eq. (D6)].

Scalar leptoquarks contribute to the  $D^0 - \bar{D}^0$  mass difference [45,82]

$$\Delta^S m_{D^0} = \frac{2}{3} m_D f_D^2 B_D \frac{(\lambda_{L,R}^{(cl)} (\lambda_{L,R}^{(ul)})^*)^2}{64\pi^2 M^2} \quad (F1)$$

(times 2 for  $S_2|_L$  and times 5 for  $S_3$ ). While constraints from  $|\Delta C| = 1$  transitions scale as  $\lambda\lambda^*/M^2$ , the ones from mixing behave differently, as  $(\lambda\lambda^*)^2/M^2$ . In our analysis we neglect the SM contribution [83,84].

Matching onto the nuclear weak charge [85]

$$Q_w(Z, N) = -2((2Z + N)C_{1u} + (2N + Z)C_{1d}), \quad (F2)$$

where  $Z$  is the proton number and  $N$  is the neutron number, we find

TABLE XII. Scalar  $SU(2)$ -singlet and -doublet leptoquark constraints for real couplings scaling as  $\text{TeV}/M$  and  $\sqrt{\text{TeV}/M}$  for  $\Delta m_{D^0}$ . Additionally,  $|\text{Im}[\lambda_L^{(u\mu)}(\lambda_R^{(u\mu)})^*]| \lesssim 3 \times 10^{-7}$  and  $|\text{Im}[\lambda_L^{(ce)}(\lambda_R^{(ce)})^*]| \lesssim 3 \times 10^{-10}$  from bounds on neutron and electron electric dipole moments.

Couplings/Mass	Constraint	Observable
$ \lambda_{S_1 L}^{(ue)} $	$\lesssim 9 \times 10^{-2}$	$V_{ud}$
$\lambda_L^{(ue)} \lambda_R^{(ue)}$	$\sim [-0.08, 0.8]$	Nuclear beta decay
$ \lambda_L^{(ue)} \lambda_R^{(u\mu)} $	$\lesssim 9 \times 10^{-2}$	$\pi^+ \rightarrow \mu^+ \nu_e$
$ \lambda_{\{L,R\}}^{(ue)} \lambda_{\{L,R\}}^{(ce)} $	$\lesssim 1 \times 10^{-1}$	$D^+ \rightarrow \pi^+ e^+ e^-$
$ \lambda_{\{L,R\}}^{(ue)} \lambda_{\{L,R\}}^{(c\mu)} $	$\lesssim 2 \times 10^{-1}$	$D^+ \rightarrow \pi^+ e^+ \mu^-$
$ \lambda_{\{L,R\}}^{(u\mu)} \lambda_{\{L,R\}}^{(ce)} $	$\lesssim 2 \times 10^{-1}$	$D^+ \rightarrow \pi^+ e^- \mu^+$
$ \lambda_{\{L,R\}}^{(u\mu)} \lambda_{\{L,R\}}^{(c\mu)} $	$\lesssim 2 \times 10^{-2}$	$D^+ \rightarrow \pi^+ \mu^+ \mu^-$
$\lambda_L^{(ce)} \lambda_R^{(ce)}$	$\sim [-0.005, 0.05]$	$D_s^+ \rightarrow \mu^+ \nu_\mu$
$\lambda_{S_1 L}^{(ce)} \lambda_{S_1 R}^{(ce)}$	$\sim [-0.01, 0.00]$	$\Delta a_e$
$\lambda_{S_2 L}^{(ce)} \lambda_{S_2 R}^{(ce)}$	$\sim [0.00, 0.01]$	
$\lambda_{S_1 L}^{(c\mu)} \lambda_{S_1 R}^{(c\mu)}$	$\sim [0.1, 0.2]$	$\Delta a_\mu$
$\lambda_{S_2 L}^{(c\mu)} \lambda_{S_2 R}^{(c\mu)}$	$\sim [-0.2, -0.1]$	
$(- \lambda_{S_1 L, S_2 L}^{(ue)} ^2 +  \lambda_{S_1 R, S_2 R}^{(ue)} ^2 +  \lambda_{S_2 R}^{(ue)} ^2)^{1/2}$	$\sim [0.2, 0.4]$	$Q_w(\text{Cs})$
$(\lambda_L^{(ue)} \lambda_R^{(ue)} - 0.02 \lambda_L^{(u\mu)} \lambda_R^{(u\mu)})$		$\Delta R_{e/\mu}$
$-0.0002( \lambda_{S_1 L}^{(ue)} ^2 -  \lambda_{S_1 L}^{(u\mu)} ^2)$	$\sim [-0.00001, -0.000003]$	
$(\lambda_{S_1 L, S_2 R}^{(ue)} \lambda_{S_1 R, S_2 L}^{(ce)} - 0.02 \lambda_{S_1 L}^{(ue)} \lambda_{S_1 L}^{(ce)})$	$\sim [-0.009, 0.01]$	$D^+ \rightarrow \mu^+ \nu_\mu$
$ \lambda_L^{(ue)} \lambda_R^{(ce)} \pm \lambda_R^{(ue)} \lambda_L^{(ce)} $	$\lesssim 1 \times 10^{-2}$	$D^0 \rightarrow e^+ e^-$
$\lambda_{L,R}^{(ue)} \lambda_{L,R}^{(ce)} + \lambda_{L,R}^{(u\mu)} \lambda_{L,R}^{(c\mu)}$	$\sim [0, 0.01]$	$\Delta m_{D^0}$
$ \lambda_{S_1 L, S_1 R}^{(qe)} \lambda_{S_1 L, S_1 R}^{(q\mu)} $	$\lesssim 1 \times 10^{-3}$	$\mu^- \rightarrow e^- \gamma$
$ \lambda_{S_2 L, S_2 R}^{(qe)} \lambda_{S_2 L, S_2 R}^{(q\mu)} $	$\lesssim 5 \times 10^{-4}$	
$ \lambda_{L,R}^{(ce)} \lambda_{R,L}^{(c\mu)} $	$\lesssim 3 \times 10^{-6}$	
$ \lambda_{L,R}^{(ue)} \lambda_{L,R}^{(u\mu)} $	$\lesssim 9 \times 10^{-7}$	$\mu - e(\text{Au})$
$ \lambda_{S_2 R}^{(ue)} \lambda_{S_2 R}^{(u\mu)} $	$\lesssim 7 \times 10^{-7}$	
$ \lambda_{L,R}^{(ue)} \lambda_{R,L}^{(u\mu)} $	$\lesssim 4 \times 10^{-7}$	
$ \lambda_{S_1 L, S_1 R}^{(ce)} \lambda_{S_1 L, S_1 R}^{(c\mu)} $	$\lesssim 9 \times 10^{-3}$	
$ \lambda_{S_2 L, S_2 R}^{(ce)} \lambda_{S_2 L, S_2 R}^{(c\mu)} $	$\lesssim 3 \times 10^{-3}$	
$ \lambda_{L,R}^{(ce)} \lambda_{R,L}^{(c\mu)} $	$\lesssim 1 \times 10^{-5}$	
$ \lambda_{L,R}^{(ue)} \lambda_{L,R}^{(u\mu)} $	$\lesssim 1 \times 10^{-3}$	$\mu^- \rightarrow e^- e^+ e^-$
$ \lambda_{S_2 R}^{(ue)} \lambda_{S_2 R}^{(u\mu)} $	$\lesssim 3 \times 10^{-3}$	

(Table continued)

TABLE XII. (Continued)

Couplings/Mass	Constraint	Observable
$ \lambda_{L,R}^{(ue)} \lambda_{R,L}^{(u\mu)} $	$\lesssim 1 \times 10^{-2}$	
$ \lambda_{L,R}^{(ce)} \lambda_{L,R}^{(c\mu)} $	$\lesssim 3 \times 10^{-3}$	
$ \lambda_{S_2 R}^{(ce)} \lambda_{S_2 R}^{(c\mu)} $	$\lesssim 6 \times 10^{-3}$	
$ \lambda_{S_1 L, S_1 R}^{(ce)} \lambda_{S_1 R, S_1 L}^{(c\mu)} $	$\lesssim 6 \times 10^{-5}$	
$ \lambda_{S_2 L, S_2 R}^{(ce)} \lambda_{S_2 R, S_2 L}^{(c\mu)} $	$\lesssim 5 \times 10^{-5}$	
$ \lambda_{L,R}^{(ue)} \lambda_{L,R}^{(c\mu)} + \lambda_{L,R}^{(u\mu)} \lambda_{L,R}^{(ce)} $	$\lesssim 8 \times 10^{-1}$	$D^0 \rightarrow \mu^\pm e^\mp$
$ \lambda_{L,R}^{(ue)} \lambda_{R,L}^{(c\mu)} + \lambda_{L,R}^{(u\mu)} \lambda_{R,L}^{(ce)} $	$\lesssim 1 \times 10^{-2}$	
$ \lambda_L^{(u\mu)} \lambda_L^{(c\mu)} + \lambda_R^{(u\mu)} \lambda_R^{(c\mu)} $	$\lesssim 6 \times 10^{-2}$	$D^0 \rightarrow \mu^+ \mu^-$
$ \lambda_L^{(u\mu)} \lambda_R^{(c\mu)} \pm \lambda_R^{(u\mu)} \lambda_L^{(c\mu)} $	$\lesssim 4 \times 10^{-3}$	

$$\begin{aligned}
 \delta_{S_1} C_{1u} &= \delta_{S_2} C_{1u} = -\frac{\sqrt{2}}{8G_F} \frac{|\lambda_R^{(ue)}|^2 - |\lambda_L^{(ue)}|^2}{M^2}, \\
 \delta_{S_2} C_{1d} &= -\frac{\sqrt{2}}{8G_F} \frac{|\lambda_{S_2 R}^{(ue)}|^2}{M^2}, \\
 \delta_{S_3} C_{1u} &= \frac{1}{2} \delta_{S_3} C_{1d} = \frac{\sqrt{2}}{8G_F} \frac{|\lambda_{S_3}^{(ue)}|^2}{M^2}, \\
 \delta_{\tilde{V}_1} C_{1u} &= \delta_{\tilde{V}_2} C_{1u} = \frac{\sqrt{2}}{4G_F} \frac{|\lambda_{\tilde{V}_{1,2}}^{(ue)}|^2}{M^2}, \\
 \delta_{V_3} C_{1u} &= -\frac{\sqrt{2}}{2G_F} \frac{|\lambda_{V_3}^{(ue)}|^2}{M^2}, \\
 \delta_{V_3} C_{1d} &= -\frac{\sqrt{2}}{4G_F} \frac{|\lambda_{V_3}^{(ue)}|^2}{M^2}. \tag{F3}
 \end{aligned}$$

We do not match  $V_2$  due to an additional  $d_R$ -quark coupling [45].

The shift in the anomalous magnetic moment of a fermion  $f$  due to a scalar LQ reads [86]

$$\begin{aligned}
 \Delta^S a_f &= -\frac{3m_f}{16\pi^2} \frac{1}{M^2} \left( m_f (|\lambda_L^{(ff')}|^2 + |\lambda_R^{(ff')}|^2) \right. \\
 &\quad \times \left( \frac{1}{3} Q_e^{(f')} - \frac{1}{6} Q_e \right) \\
 &\quad + m_f \text{Re}[\lambda_L^{(ff')} (\lambda_R^{(ff')})^*] \\
 &\quad \times \left( \left( -3 - 2 \ln \frac{m_{f'}^2}{M^2} \right) Q_e^{(f')} - Q_e \right) \Big). \tag{F4}
 \end{aligned}$$

Here,  $Q_e$  and  $Q_e^{(f')}$  denote the electric charges of the leptoquark and the fermion  $f'$  in the loop, respectively.

The contribution to the electric dipole moment of  $f$  reads [86]

$$\begin{aligned}
 d_f &= \frac{e}{32\pi^2} \frac{1}{M^2} m_f \text{Im}[\lambda_L^{(ff')} (\lambda_R^{(ff')})^*] \\
 &\quad \times \left( \left( -3 - 2 \ln \frac{m_{f'}^2}{M^2} \right) Q_e^{(f')} - Q_e \right), \tag{F5}
 \end{aligned}$$

TABLE XIII. Scalar  $SU(2)$ -triplet leptoquark constraints for real couplings scaling as  $\text{TeV}/M$  and  $\sqrt{\text{TeV}/M}$  for  $\Delta m_{D^0}$ . For the constraint from the weak charge we apply its  $2\sigma$  interval.

Couplings/Mass	Constraint	Observable
$ \lambda^{(ue)} $	$\lesssim 0.1$	$Q_w(\text{Cs})$
$ \lambda^{(ue)} $	$\lesssim 9 \times 10^{-2}$	$V_{ud}$
$\lambda^{(ue)} \lambda^{(ce)}$	$\sim [-0.6, 1]$	$D^+ \rightarrow \mu^+ \nu_\mu$
$ \lambda^{(ue)} \lambda^{(ce)} $	$\lesssim 1 \times 10^{-1}$	$D^+ \rightarrow \pi^+ e^+ e^-$
$ \lambda^{(ue)} \lambda^{(c\mu)} $	$\lesssim 2 \times 10^{-1}$	$D^+ \rightarrow \pi^+ e^+ \mu^-$
$ \lambda^{(u\mu)} \lambda^{(ce)} $	$\lesssim 3 \times 10^{-1}$	$D^+ \rightarrow \pi^+ e^- \mu^+$
$ \lambda^{(u\mu)} \lambda^{(c\mu)} $	$\lesssim 1 \times 10^{-2}$	$D^+ \rightarrow \pi^+ \mu^+ \mu^-$
$ \lambda^{(u\mu)} \lambda^{(c\mu)} $	$\lesssim 6 \times 10^{-2}$	$D^0 \rightarrow \mu^+ \mu^-$
$(- \lambda^{(ue)} ^2 +  \lambda^{(u\mu)} ^2)^{1/2}$	$\sim [0.2, 0.4]$	$\Delta R_{e/\mu}$
$ \lambda^{(ue)} \lambda^{(u\mu)} + \lambda^{(ce)} \lambda^{(c\mu)} $	$\lesssim 5 \times 10^{-4}$	$\mu^- \rightarrow e^- \gamma$
$(\lambda^{(ue)} \lambda^{(ce)} + \lambda^{(u\mu)} \lambda^{(c\mu)})$	$\sim [0, 0.007]$	$\Delta m_{D^0}$
$ \lambda^{(ue)} \lambda^{(c\mu)} + \lambda^{(u\mu)} \lambda^{(ce)} $	$\lesssim 8 \times 10^{-1}$	$D^0 \rightarrow \mu^\pm e^\mp$
$ \lambda^{(ue)} \lambda^{(u\mu)} $	$\lesssim 7 \times 10^{-7}$	$\mu - e(\text{Au})$
$ \lambda^{(ce)} \lambda^{(c\mu)} $	$\lesssim 9 \times 10^{-3}$	
$ \lambda^{(ue)} \lambda^{(u\mu)} $	$\lesssim 1 \times 10^{-2}$	$\mu^- \rightarrow e^- e^+ e^-$
$ \lambda^{(ce)} \lambda^{(c\mu)} $	$\lesssim 6 \times 10^{-3}$	

TABLE XIV. Vector leptoquark constraints for real couplings scaling as  $\text{TeV}/M$ . For the constraint on  $\tilde{V}_{1,2}$  from  $Q_w$  we apply its  $2\sigma$  interval. For  $V_3$  all constraints have to be multiplied by a factor of  $1/2$ .

Couplings/Mass	Constraint	Observable
$ \lambda_{\tilde{V}_{1,2}}^{(ue)} $	$\lesssim 0.1$	$Q_w(\text{Cs})$
$ \lambda_{V_3}^{(ue)} $	$\sim 0.1$	
$ \lambda_{V_3}^{(ue)} $	$\lesssim 6 \times 10^{-2}$	$V_{ud}$
$\lambda_{V_3}^{(ue)} \lambda_{V_3}^{(ce)}$	$\sim [-0.3, 0.5]$	$D^+ \rightarrow \mu^+ \nu_\mu$
$ \lambda^{(ue)} \lambda^{(ce)} $	$\lesssim 6 \times 10^{-2}$	$D^+ \rightarrow \pi^+ e^+ e^-$
$ \lambda^{(ue)} \lambda^{(c\mu)} $	$\lesssim 1 \times 10^{-1}$	$D^+ \rightarrow \pi^+ e^+ \mu^-$
$ \lambda^{(u\mu)} \lambda^{(ce)} $	$\lesssim 1 \times 10^{-1}$	$D^+ \rightarrow \pi^+ e^- \mu^+$
$ \lambda^{(u\mu)} \lambda^{(c\mu)} $	$\lesssim 1 \times 10^{-2}$	$D^+ \rightarrow \pi^+ \mu^+ \mu^-$
$ \lambda^{(u\mu)} \lambda^{(c\mu)} $	$\lesssim 3 \times 10^{-2}$	$D^0 \rightarrow \mu^+ \mu^-$
$(- \lambda_{V_3}^{(ue)} ^2 +  \lambda_{V_3}^{(u\mu)} ^2)^{1/2}$	$\sim [0.2, 0.3]$	$\Delta R_{e/\mu}$
$ \lambda^{(ue)} \lambda^{(c\mu)} + \lambda^{(u\mu)} \lambda^{(ce)} $	$\lesssim 4 \times 10^{-1}$	$D^0 \rightarrow \mu^\pm e^\mp$
$ \lambda^{(qe)} \lambda^{(q\mu)} $	$\lesssim 1 \times 10^{-4}$	$\mu^- \rightarrow e^- \gamma$
$ \lambda_{V_3}^{(qe)} \lambda_{V_3}^{(q\mu)} $	$\lesssim 6 \times 10^{-5}$	
$ \lambda^{(ue)} \lambda^{(u\mu)} $	$\lesssim 7 \times 10^{-7}$	$\mu - e(\text{Au})$
$ \lambda_{\tilde{V}_1, \tilde{V}_2}^{(ce)} \lambda_{\tilde{V}_1, \tilde{V}_2}^{(c\mu)} $	$\lesssim 1 \times 10^{-2}$	
$ \lambda_{V_2}^{(ce)} \lambda_{V_2}^{(c\mu)} $	$\lesssim 6 \times 10^{-3}$	
$ \lambda_{V_3}^{(ce)} \lambda_{V_3}^{(c\mu)} $	$\lesssim 7 \times 10^{-3}$	
$ \lambda^{(ue)} \lambda^{(u\mu)} $	$\lesssim 4 \times 10^{-4}$	$\mu^- \rightarrow e^- e^+ e^-$
$ \lambda_{V_3}^{(ue)} \lambda_{V_3}^{(u\mu)} $	$\lesssim 2 \times 10^{-4}$	
$ \lambda_{\tilde{V}_1, \tilde{V}_2}^{(ce)} \lambda_{\tilde{V}_1, \tilde{V}_2}^{(c\mu)} $	$\lesssim 8 \times 10^{-4}$	
$ \lambda_{V_2}^{(ce)} \lambda_{V_2}^{(c\mu)} $	$\lesssim 6 \times 10^{-4}$	
$ \lambda_{V_3}^{(ce)} \lambda_{V_3}^{(c\mu)} $	$\lesssim 3 \times 10^{-4}$	

times 3 for color if  $f'$  is a quark. For electrons  $|d_e^{\text{SM}}| \leq 10^{-38} e \text{ cm}$  [87]. The neutron electric dipole moment receives contributions from quarks  $d_n = 4/3d_d - 1/3d_u$ , with  $d_n^{\text{SM}} \sim \mathcal{O}(10^{-34}) e \text{ cm}$  [88].

The lepton flavor-violating radiative muon decay in the case of a scalar LQ is [89]

TABLE XV. Constraints on the leptoquark coupling products from kaon decays [54] scaling as  $\text{TeV}/M$ .

Couplings/Mass	Constraint	Observable
$ \lambda_{S_1 L}^{(ul)} \lambda_{S_1 L}^{(cl')} $	$\lesssim 4 \times 10^{-4}$	$(K^+ \rightarrow \pi^+ \bar{\nu} \nu)/(K^+ \rightarrow \pi^0 \bar{e} \nu_e)$
$ \lambda_{S_2 R}^{(ue)} \lambda_{S_2 R}^{(ce)} $	$\lesssim 2 \times 10^{-3}$	$K_L^0 \rightarrow \bar{e} e$
$ \lambda_{S_2 R}^{(u\mu)} \lambda_{S_2 R}^{(ce)} $	$\lesssim 1 \times 10^{-5}$	$K_L^0 \rightarrow \bar{e} \mu$
$ \lambda_{S_2 R}^{(u\mu)} \lambda_{S_2 R}^{(c\mu)} $	$\lesssim 3 \times 10^{-4}$	$K_L^0 \rightarrow \bar{\mu} \mu$
$ \lambda_{S_3}^{(ue)} \lambda_{S_3}^{(ce)} $	$\lesssim 4 \times 10^{-4}$	$(K^+ \rightarrow \pi^+ \bar{\nu} \nu)/(K^+ \rightarrow \pi^0 \bar{e} \nu_e)$
$ \lambda_{S_3}^{(ue)} \lambda_{S_3}^{(c\mu)} ,  \lambda_{S_3}^{(u\mu)} \lambda_{S_3}^{(ce)} $	$\lesssim 1 \times 10^{-5}$	$K_L^0 \rightarrow \bar{e} \mu$
$ \lambda_{S_3}^{(u\mu)} \lambda_{S_3}^{(c\mu)} $	$\lesssim 3 \times 10^{-4}$	$K_L^0 \rightarrow \bar{\mu} \mu$
$ \lambda_{V_2}^{(ue)} \lambda_{V_2}^{(ce)} $	$\lesssim 1 \times 10^{-3}$	$K_L^0 \rightarrow \bar{e} e$
$ \lambda_{V_2}^{(ue)} \lambda_{V_2}^{(c\mu)} ,  \lambda_{V_2}^{(u\mu)} \lambda_{V_2}^{(ce)} $	$\lesssim 5 \times 10^{-6}$	$K_L^0 \rightarrow \bar{e} \mu$
$ \lambda_{V_2}^{(u\mu)} \lambda_{V_2}^{(c\mu)} $	$\lesssim 2 \times 10^{-4}$	$K_L^0 \rightarrow \bar{\mu} \mu$
$ \lambda_{V_3}^{(ue)} \lambda_{V_3}^{(ce)} $	$\lesssim 8 \times 10^{-5}$	$(K^+ \rightarrow \pi^+ \bar{\nu} \nu)/(K^+ \rightarrow \pi^0 \bar{e} \nu_e)$
$ \lambda_{V_3}^{(ue)} \lambda_{V_3}^{(c\mu)} ,  \lambda_{V_3}^{(u\mu)} \lambda_{V_3}^{(ce)} $	$\lesssim 3 \times 10^{-6}$	$K_L^0 \rightarrow \bar{e} \mu$
$ \lambda_{V_3}^{(u\mu)} \lambda_{V_3}^{(c\mu)} $	$\lesssim 7 \times 10^{-5}$	$K_L^0 \rightarrow \bar{\mu} \mu$

$$\delta_S \mathcal{B}_{\mu \rightarrow e \gamma} = \frac{\alpha_e}{4\Gamma_\mu} m_\mu^5 (|F_{2LR}^\gamma|^2 + |F_{2RL}^\gamma|^2), \quad (\text{F6})$$

where we note the typo  $F_1 \leftrightarrow F_2$  in [89],

$$F_{2LR,2RL}^\gamma = \frac{3}{16\pi^2} \frac{1}{M^2} \left( \lambda_{L,R}^{(q\mu)} (\lambda_{L,R}^{(qe)})^* \left( \frac{1}{6} Q_e^{(q)} - \frac{1}{12} Q_e \right) - \frac{m_q}{m_\mu} \lambda_{R,L}^{(q\mu)} (\lambda_{L,R}^{(qe)})^* \left( \left( -\frac{3}{2} - \ln \frac{m_q^2}{M^2} \right) Q_e^{(q)} - \frac{1}{2} Q_e \right) \right). \quad (\text{F7})$$

In the case of a vector LQ [45]

$$\delta_V \mathcal{B}_{\mu \rightarrow e \gamma} = \frac{1}{\Gamma_\mu} \frac{m_\mu}{8\pi} (|F^V|^2 + |F^A|^2) \quad (\text{F8})$$

with

$$|F^{V,A}| = \sqrt{\alpha_e} 4\pi \frac{|\lambda^{(qe)} \lambda^{(q\mu)}|}{32\pi^2} \frac{m_\mu^2}{M^2} \left( Q_e^{(q)} 2 + Q_e \frac{5}{2} \right) \quad (\text{F9})$$

(times 2 for up-type quarks in scenario  $V_3$ ).

The lepton flavor-violating muon decay in the case of a scalar LQ is [90]

$$\begin{aligned}
 \delta_S \mathcal{B}_{\mu \rightarrow eee} = & \frac{\alpha_e^2 m_\mu^5}{32\pi\Gamma_\mu} \left( |T_{1L}|^2 + |T_{1R}|^2 + \frac{2}{3} (|T_{2L}|^2 + |T_{2R}|^2) \left( 8 \ln \frac{m_\mu}{2m_e} - 11 \right) - 4 \operatorname{Re}[T_{1L}T_{2R}^* + T_{2L}T_{1R}^*] \right. \\
 & + \frac{1}{3} (2(|Z_L g_{Ll}|^2 + |Z_R g_{Rl}|^2) + |Z_L g_{Rl}|^2 + |Z_R g_{Ll}|^2) + \frac{1}{6} (|B_{1L}|^2 + |B_{1R}|^2) + \frac{1}{3} (|B_{2L}|^2 + |B_{2R}|^2) \\
 & + \frac{2}{3} \operatorname{Re}[T_{1L}B_{1L}^* + T_{1L}B_{2L}^* + T_{1R}B_{1R}^* + T_{1R}B_{2R}^*] - \frac{4}{3} \operatorname{Re}[T_{2R}B_{1L}^* + T_{2L}B_{1R}^* + T_{2L}B_{2R}^* + T_{2R}B_{2L}^*] \\
 & + \frac{2}{3} \operatorname{Re}[B_{1L}Z_L^* g_{Ll} + B_{1R}Z_R^* g_{Rl} + B_{2L}Z_L^* g_{Rl} + B_{2R}Z_R^* g_{Ll}] + \frac{2}{3} \operatorname{Re}[2(T_{1L}Z_L^* g_{Ll} + T_{1R}Z_R^* g_{Rl}) \\
 & + T_{1L}Z_L^* g_{Rl} + T_{1R}Z_R^* g_{Ll}] + \frac{2}{3} \operatorname{Re}[-4(T_{2R}Z_L^* g_{Ll} + T_{2L}Z_R^* g_{Rl}) - 2(T_{2L}Z_R^* g_{Ll} + T_{2R}Z_L^* g_{Rl})] \left. \right), \quad (\text{F10})
 \end{aligned}$$

where we correct the typo in  $Z_{L,R}$  related terms in [90],

$$T_{1L,1R} = -\frac{3}{16\pi^2} \frac{1}{M^2} \lambda_{L,R}^{(q\mu)} (\lambda_{L,R}^{(qe)})^* \left( \left( \frac{4}{9} + \frac{1}{3} \ln \frac{m_q^2}{M^2} \right) Q_e^{(q)} + \frac{-1}{18} Q_e \right), \quad (\text{F11})$$

$$\begin{aligned}
 T_{2L,2R} = & \frac{3}{16\pi^2} \frac{1}{M^2} \left( -\left( \lambda_{R,L}^{(q\mu)} (\lambda_{R,L}^{(qe)})^* \frac{1}{6} + \frac{m_q}{m_\mu} \lambda_{R,L}^{(q\mu)} (\lambda_{L,R}^{(qe)})^* \left( -\frac{3}{2} - \ln \frac{m_q^2}{M^2} \right) \right) Q_e^{(q)} \right. \\
 & \left. + \left( \lambda_{R,L}^{(q\mu)} (\lambda_{R,L}^{(qe)})^* \frac{1}{12} + \frac{m_q}{m_\mu} \lambda_{R,L}^{(q\mu)} (\lambda_{L,R}^{(qe)})^* \frac{1}{2} \right) Q_e \right), \quad (\text{F12})
 \end{aligned}$$

$$Z_{L,R} = -\frac{3}{16\pi^2} \frac{1}{M^2} \lambda_{L,R}^{(q\mu)} (\lambda_{L,R}^{(qe)})^* \frac{1}{m_Z^2 \sin^2 \theta_w \cos^2 \theta_w} \left( m_\mu^2 \frac{3}{8} 2g_{Lq,Rq} - m_q^2 \left( 1 + \ln \frac{m_q^2}{M^2} \right) g_{Rq,Lq} + m_\mu^2 \frac{3}{8} 2(-g) \right), \quad (\text{F13})$$

$$B_{1L,1R} = \frac{3}{32\pi^2} \lambda_{L,R}^{(q\mu)} (\lambda_{L,R}^{(qe)})^* |\lambda_{L,R}^{(q'e)}|^2 \frac{-1}{M^2}, \quad (\text{F14})$$

$$B_{2L,2R} = \frac{3}{64\pi^2} \lambda_{L,R}^{(q\mu)} (\lambda_{L,R}^{(qe)})^* |\lambda_{R,L}^{(q'e)}|^2 \frac{-1}{M^2} \quad (\text{F15})$$

and

$$g_{Lf,Rf} = T_3^{(fL,fR)} - Q_e^{(f)} \sin^2 \theta_w, \quad g = T_3 - Q_e \sin^2 \theta_w \quad (\text{F16})$$

( $g_L \leftrightarrow g_R$  for  $S_2$ ). Here,  $T_3$  is the third component of the weak isospin of the LQ and  $f_{L,R}$  label chiral fermions; that is,  $g_{Lf,Rf}$  are SM couplings and  $g$  is the LQ coupling. In the case of a vector LQ [91]

$$\delta_V \mathcal{B}_{\mu \rightarrow eee} = \frac{3\alpha_e^2}{8\pi^2} (Q_e^{(q)})^2 \ln^2 \frac{m_q^2}{M^2} \frac{|\lambda^{(q\mu)} \lambda^{(qe)}|^2}{G_F^2 M^4} \quad (\text{F17})$$

(times 4 for up-type quarks in scenario  $V_3$ ), where we neglect terms  $\sim Q_e$ ,  $m_f^2/M^2$ -suppressed box diagrams and  $m_f^2/m_Z^2$ -suppressed Z diagrams.

Matching onto the  $\mu - e$  conversion in nuclei rate [92]

$$\begin{aligned}
 \Gamma_{\mu-e} = & 4m_\mu^5 \left| \frac{1}{4} C_{DR} D + C_{SL} G_S^{(u,p)} S^{(p)} + C_{SL} G_S^{(u,n)} S^{(n)} + 2C_{VR} V^{(p)} + C_{VR} V^{(n)} \right|^2 \\
 & + 4m_\mu^5 \left| \frac{1}{4} C_{DL} D + C_{SR} G_S^{(u,p)} S^{(p)} + C_{SR} G_S^{(u,n)} S^{(n)} + 2C_{VL} V^{(p)} + C_{VL} V^{(n)} \right|^2 \quad (\text{F18})
 \end{aligned}$$

we find

$$\begin{aligned}
\delta_S C_{VR} &= -\frac{\lambda_R^{(ue)}(\lambda_R^{(u\mu)})^*}{4M^2}, & \delta_S C_{VL} &= -\frac{\lambda_L^{(ue)}(\lambda_L^{(u\mu)})^*}{4M^2}, & \delta_S C_{SR} &= -\frac{\lambda_L^{(ue)}(\lambda_R^{(u\mu)})^*}{4M^2}, & \delta_S C_{SL} &= -\frac{\lambda_R^{(ue)}(\lambda_L^{(u\mu)})^*}{4M^2}, \\
\delta_S C_{DR,DL} &= \frac{1}{2m_\mu} F_{2RL,2LR}^\gamma, & \delta_{\tilde{V}_1} C_{VR} &= \frac{\lambda_{\tilde{V}_1}^{(ue)}(\lambda_{\tilde{V}_1}^{(u\mu)})^*}{2M^2}, & \delta_{V_2} C_{VR} &= \frac{\lambda_{V_2}^{(u\mu)}(\lambda_{V_2}^{(ue)})^*}{2M^2}, & \delta_{\tilde{V}_2} C_{VL} &= \frac{\lambda_{\tilde{V}_2}^{(u\mu)}(\lambda_{\tilde{V}_2}^{(ue)})^*}{2M^2}, \\
\delta_{V_3} C_{VL} &= \frac{\lambda_{V_3}^{(ue)}(\lambda_{V_3}^{(u\mu)})^*}{M^2}, & \delta_{\tilde{V}_1, V_2} C_{DR,DL} &= -\frac{1}{4m_\mu^2 \sqrt{\alpha_e} 4\pi} (|F^V| \pm |F^A|), & \delta_{\tilde{V}_2, V_3} C_{DR,DL} &= -\frac{1}{4m_\mu^2 \sqrt{\alpha_e} 4\pi} (|F^V| \mp |F^A|),
\end{aligned} \tag{F19}$$

where  $F_{2RL}^\gamma$  are given by Eq. (F7) and  $|F^{V,A}|$  are given by Eq. (F9) (times 2 for up-type quarks in scenario  $V_3$ ). We neglect loop-suppressed gluonic interactions. The nucleon form factors are given as  $G_S^{(u,p)} = 5.1$  and  $G_S^{(u,n)} = 4.3$  [92], and we take the overlap integrals of muons and electrons weighted by proton and neutron densities for titanium and gold,

$$\begin{aligned}
D_{\text{Ti}} &= 0.0864, & S_{\text{Ti}}^{(p)} &= 0.0368, & S_{\text{Ti}}^{(n)} &= 0.0435, & V_{\text{Ti}}^{(p)} &= 0.0396, & V_{\text{Ti}}^{(n)} &= 0.0468, \\
D_{\text{Au}} &= 0.189, & S_{\text{Au}}^{(p)} &= 0.0614, & S_{\text{Au}}^{(n)} &= 0.0918, & V_{\text{Au}}^{(p)} &= 0.0974, & V_{\text{Au}}^{(n)} &= 0.146.
\end{aligned} \tag{F20}$$

Matching onto the leptonic pseudoscalar decay rate [93]

$$\Gamma_{P \rightarrow l\nu} = \frac{G_F^2 f_P^2 (m_P^2 - m_l^2)^2}{8\pi m_P^3} \left| m_l V_{qq'} + m_l \frac{\sqrt{2}}{4G_F} (C_{VRL} - C_{VLL}) + \frac{m_P^2}{m_q + m_{q'}} \frac{\sqrt{2}}{4G_F} (C_{SLR} - C_{SRR}) \right|^2 \tag{F21}$$

we find

$$\begin{aligned}
\delta_{S_1} C_{VLL} &= \frac{1}{2} \frac{\lambda_{S_1 L}^{(ql)}(\lambda_{S_1 L}^{(q'l)})^*}{M^2}, & \delta_{S_1} C_{SRR} &= -\frac{1}{2} \frac{\lambda_{S_1 R}^{(ql)}(\lambda_{S_1 R}^{(q'l)})^*}{M^2}, & \delta_{S_2} C_{SRR} &= \frac{1}{2} \frac{\lambda_{S_2 R}^{(q'l)}(\lambda_{S_2 R}^{(ql)})^*}{M^2}, \\
\delta_{S_3} C_{VLL} &= -\frac{1}{2} \frac{\lambda_{S_3}^{(ql)}(\lambda_{S_3}^{(q'l)})^*}{M^2}, & \delta_{V_3} C_{VLL} &= -\frac{\lambda_{V_3}^{(q'l)}(\lambda_{V_3}^{(ql)})^*}{M^2}.
\end{aligned} \tag{F22}$$

We do not match  $V_2$  due to an additional  $d_L$ -quark coupling [45].

We deduce the shift in  $R_{e/\mu} = \Gamma_{\pi \rightarrow e\nu_e} / \Gamma_{\pi \rightarrow \mu\nu_\mu}$ ,

$$\delta_{LQ} R_{e/\mu} = R_{e/\mu}^{\text{SM}} \frac{1}{\sqrt{2} G_F V_{ud}} \text{Re} \left[ (C_{VRL}^{(l=e)} - C_{VLL}^{(l=e)}) - (C_{VRL}^{(l=\mu)} - C_{VLL}^{(l=\mu)}) + \frac{m_\pi^2}{m_u + m_d} \left( \frac{C_{SLR}^{(l=e)} - C_{SRR}^{(l=e)}}{m_e} - \frac{C_{SLR}^{(l=\mu)} - C_{SRR}^{(l=\mu)}}{m_\mu} \right) \right], \tag{F23}$$

and the shift in the CKM parameter

$$\frac{\Delta^{LQ} V_{ud}}{V_{ud}} = \frac{\sqrt{2}}{4G_F} C_{VLL}^{(ue)} \tag{F24}$$

by means of quark beta decay normalized to muon decay.

We match onto nuclear beta decay parameters to constrain Wilson coefficients [94],

$$-0.14 \times 10^{-2} < \frac{G_F \alpha_e C_T + C_{T5}}{\sqrt{2}\pi C_A} < 1.4 \times 10^{-2} \quad (90\% \text{CL}), \tag{F25}$$

where  $C_A^{\text{SM}} = -1.27 G_F V_{ud}$ .

We obtain no constraints better than  $|\lambda| \lesssim M/\text{TeV}$  from the decay  $\pi^0 \rightarrow \mu e$ ,  $\Delta m_D$  via vector LQs [21], the  $D^0 - \bar{D}^0$  lifetime difference [95,96], the anomalous magnetic moment via vector LQs [97], the decay  $Z \rightarrow ff$  via scalar LQs [98], the decay  $Z \rightarrow e\mu$  via scalar LQs [89], triple correlation coefficients in nuclear beta decay [99–101] nor additional nuclear beta decay parameters [102].

- [1] T. Blake, T. Gershon, and G. Hiller, *Annu. Rev. Nucl. Part. Sci.* **65**, 113 (2015).
- [2] J. L. Hewett *et al.*, [arXiv:hep-ph/0503261](https://arxiv.org/abs/hep-ph/0503261).
- [3] D. M. Asner *et al.*, *Int. J. Mod. Phys. A* **24**, 499 (2009).
- [4] T. Aushev *et al.*, [arXiv:1002.5012](https://arxiv.org/abs/1002.5012).
- [5] B. O'Leary *et al.* (SuperB Collaboration), [arXiv:1008.1541](https://arxiv.org/abs/1008.1541).
- [6] I. Dorner, S. Fajfer, N. Konik, and I. Niandic, *J. High Energy Phys.* **11** (2013) 084.
- [7] G. Hiller and M. Schmaltz, *Phys. Rev. D* **90**, 054014 (2014).
- [8] B. Gripaios, M. Nardecchia, and S. A. Renner, *J. High Energy Phys.* **05** (2015) 006.
- [9] L. Calibbi, A. Crivellin, and T. Ota, *Phys. Rev. Lett.* **115**, 181801 (2015).
- [10] M. Freytsis, Z. Ligeti, and J. T. Ruderman, *Phys. Rev. D* **92**, 054018 (2015).
- [11] S. de Boer, B. Müller, and D. Seidel, Report Nos. DO-TH15/11, QFET-2015-27.
- [12] C. Greub, T. Hurth, M. Misiak, and D. Wyler, *Phys. Lett. B* **382**, 415 (1996).
- [13] S. Fajfer, P. Singer, and J. Zupan, *Eur. Phys. J. C* **27**, 201 (2003).
- [14] K. G. Chetyrkin, M. Misiak, and M. Munz, *Phys. Lett. B* **400**, 206 (1997); **425**, 414 (1998).
- [15] C. Bobeth, M. Misiak, and J. Urban, *Nucl. Phys.* **B574**, 291 (2000).
- [16] P. Gambino, M. Gorbahn, and U. Haisch, *Nucl. Phys.* **B673**, 238 (2003).
- [17] M. Gorbahn and U. Haisch, *Nucl. Phys.* **B713**, 291 (2005).
- [18] G. Burdman, E. Golowich, J. L. Hewett, and S. Pakvasa, *Phys. Rev. D* **66**, 014009 (2002).
- [19] A. Paul, I. I. Bigi, and S. Recksiegel, *Phys. Rev. D* **83**, 114006 (2011).
- [20] R. M. Wang, J. H. Sheng, J. Zhu, Y. Y. Fan, and Y. G. Xu, *Int. J. Mod. Phys. A* **30**, 1550063 (2015).
- [21] T. Inami and C. S. Lim, *Prog. Theor. Phys.* **65**, 297 (1981); **65**, 1772 (1981).
- [22] M. Czakon, U. Haisch, and M. Misiak, *J. High Energy Phys.* **03** (2007) 008.
- [23] M. Gorbahn, U. Haisch, and M. Misiak, *Phys. Rev. Lett.* **95**, 102004 (2005).
- [24] A. J. Buras and M. Munz, *Phys. Rev. D* **52**, 186 (1995).
- [25] C. Greub, V. Pilipp, and C. Schubach, *J. High Energy Phys.* **12** (2008) 040.
- [26] Y. Amhis *et al.* (Heavy Flavor Averaging Group (HFAG) Collaboration), [arXiv:1412.7515](https://arxiv.org/abs/1412.7515).
- [27] R. Aaij *et al.* (LHCb Collaboration), *Phys. Lett. B* **724**, 203 (2013).
- [28] C. Bobeth, P. Gambino, M. Gorbahn, and U. Haisch, *J. High Energy Phys.* **04** (2004) 071.
- [29] T. Huber, E. Lunghi, M. Misiak, and D. Wyler, *Nucl. Phys.* **B740**, 105 (2006).
- [30] S. Fajfer and S. Prelovsek, *Phys. Rev. D* **73**, 054026 (2006).
- [31] K. A. Olive *et al.* (Particle Data Group Collaboration), *Chin. Phys. C* **38**, 090001 (2014).
- [32] L. G. Landsberg, *Phys. Rep.* **128**, 301 (1985).
- [33] L. Cappiello, O. Cata, and G. D'Ambrosio, *J. High Energy Phys.* **04** (2013) 135.
- [34] C. Bobeth, G. Hiller, and G. Piranishvili, *J. High Energy Phys.* **12** (2007) 040.
- [35] S. Fajfer and N. Konik, *Phys. Rev. D* **87**, 054026 (2013).
- [36] S. Fajfer, [arXiv:1509.01997](https://arxiv.org/abs/1509.01997).
- [37] S. Fajfer, S. Prelovsek, and P. Singer, *Phys. Rev. D* **64**, 114009 (2001).
- [38] S. Fajfer, N. Kosnik, and S. Prelovsek, *Phys. Rev. D* **76**, 074010 (2007).
- [39] C. Delaunay, J. F. Kamenik, G. Perez, and L. Randall, *J. High Energy Phys.* **01** (2013) 027.
- [40] A. Paul, A. De La Puente, and I. I. Bigi, *Phys. Rev. D* **90**, 014035 (2014).
- [41] I. Dorsner, S. Fajfer, and N. Kosnik, *Phys. Rev. D* **86**, 015013 (2012).
- [42] W. Buchmüller, R. Ruckl, and D. Wyler, *Phys. Lett. B* **191**, 442 (1987); **448**, 320 (1999).
- [43] S. Fajfer and N. Kosnik, *Phys. Rev. D* **79**, 017502 (2009).
- [44] S. Davidson and S. Descotes-Genon, *J. High Energy Phys.* **11** (2010) 073.
- [45] S. Davidson, D. C. Bailey, and B. A. Campbell, *Z. Phys. C* **61**, 613 (1994).
- [46] A. M. Baldini *et al.*, [arXiv:1301.7225](https://arxiv.org/abs/1301.7225).
- [47] Y. G. Cui *et al.* (COMET Collaboration), Report No. KEK-2009-10.
- [48] L. Bartoszek *et al.* (Mu2e Collaboration), [arXiv:1501.05241](https://arxiv.org/abs/1501.05241).
- [49] I. de Medeiros Varzielas and G. Hiller, *J. High Energy Phys.* **06** (2015) 072.
- [50] I. de Medeiros Varzielas and G. G. Ross, *Nucl. Phys.* **B733**, 31 (2006).
- [51] G. Altarelli and F. Feruglio, *Nucl. Phys.* **B741**, 215 (2006).
- [52] C. D. Froggatt and H. B. Nielsen, *Nucl. Phys.* **B147**, 277 (1979).
- [53] J. F. Kamenik and C. Smith, *Phys. Lett. B* **680**, 471 (2009).
- [54] M. Carpentier and S. Davidson, *Eur. Phys. J. C* **70**, 1071 (2010).
- [55] S. Fajfer and N. Konik, *Eur. Phys. J. C* **75**, 567 (2015).
- [56] R. Aaij *et al.* (LHCb Collaboration), *Phys. Lett. B* **754**, 167 (2016).
- [57] M. Ablikim *et al.* (BESIII Collaboration), *Phys. Rev. Lett.* **116**, 082001 (2016).
- [58] K. G. Chetyrkin, J. H. Kuhn, and M. Steinhauser, *Comput. Phys. Commun.* **133**, 43 (2000).
- [59] UTfit Collaboration, <http://www.utfit.org/UTfit>.
- [60] D. M. Asner *et al.* (CLEO Collaboration), *Phys. Rev. D* **81**, 052007 (2010).
- [61] S. Aoki *et al.*, *Eur. Phys. J. C* **74**, 2890 (2014).
- [62] N. Carrasco, P. Dimopoulos, R. Frezzotti, V. Lubicz, G. C. Rossi, S. Simula, and C. Tarantino (ETM Collaboration), *Phys. Rev. D* **92**, 034516 (2015).
- [63] S. G. Porsev, K. Beloy, and A. Derevianko, *Phys. Rev. D* **82**, 036008 (2010).
- [64] V. A. Dzuba, J. C. Berengut, V. V. Flambaum, and B. Roberts, *Phys. Rev. Lett.* **109**, 203003 (2012).
- [65] V. Cirigliano and I. Rosell, *Phys. Rev. Lett.* **99**, 231801 (2007).
- [66] T. Aoyama, M. Hayakawa, T. Kinoshita, and M. Nio, *Phys. Rev. D* **91**, 033006 (2015).
- [67] T. Suzuki, D. F. Measday, and J. P. Roalsvig, *Phys. Rev. C* **35**, 2212 (1987).

- [68] C. Greub, T. Hurth, and D. Wyler, *Phys. Rev. D* **54**, 3350 (1996).
- [69] N. Isgur and M. B. Wise, *Phys. Rev. D* **42**, 2388 (1990).
- [70] J. Charles, A. Le Yaouanc, L. Oliver, O. Pene, and J. C. Raynal, *Phys. Rev. D* **60**, 014001 (1999).
- [71] C. Bobeth, G. Hiller, D. van Dyk, and C. Wacker, *J. High Energy Phys.* **01** (2012) 107.
- [72] M. Beneke and T. Feldmann, *Nucl. Phys.* **B592**, 3 (2001).
- [73] J. Koponen, [arXiv:1311.6931](https://arxiv.org/abs/1311.6931).
- [74] S. Fukae, C. S. Kim, T. Morozumi, and T. Yoshikawa, *Phys. Rev. D* **59**, 074013 (1999).
- [75] A. Ghinculov, T. Hurth, G. Isidori, and Y. P. Yao, *Nucl. Phys.* **B685**, 351 (2004).
- [76] I. R. Blokland, A. Czarnecki, M. Slusarczyk, and F. Tkachov, *Phys. Rev. D* **71**, 054004 (2005); **79**, 019901 (2009).
- [77] A. Pak and A. Czarnecki, *Phys. Rev. D* **78**, 114015 (2008).
- [78] A. Ali, G. Hiller, L. T. Handoko, and T. Morozumi, *Phys. Rev. D* **55**, 4105 (1997).
- [79] G. Buchalla and G. Isidori, *Nucl. Phys.* **B525**, 333 (1998).
- [80] G. Aad *et al.* (ATLAS Collaboration), *Eur. Phys. J. C* **76**, 5 (2016).
- [81] CMS Collaboration, Report No. CMS-PAS-EXO-12-042.
- [82] J. P. Saha, B. Misra, and A. Kundu, *Phys. Rev. D* **81**, 095011 (2010).
- [83] E. Golowich and A. A. Petrov, *Phys. Lett. B* **625**, 53 (2005).
- [84] A. A. Petrov, [arXiv:1312.5304](https://arxiv.org/abs/1312.5304).
- [85] M. I. Gresham, I. W. Kim, S. Tulin, and K. M. Zurek, *Phys. Rev. D* **86**, 034029 (2012).
- [86] K. Cheung, *Phys. Rev. D* **64**, 033001 (2001).
- [87] M. E. Pospelov and I. B. Khriplovich, *Yad. Fiz.* **53**, 1030 (1991) [*Sov. J. Nucl. Phys.* **53**, 638 (1991)].
- [88] A. Czarnecki and B. Krause, *Phys. Rev. Lett.* **78**, 4339 (1997).
- [89] R. Benbrik and C. K. Chua, *Phys. Rev. D* **78**, 075025 (2008).
- [90] R. Benbrik, M. Chabab, and G. Faisel, [arXiv:1009.3886](https://arxiv.org/abs/1009.3886).
- [91] A. A. Gvozdev, A. V. Kuznetsov, N. V. Mikheev, and L. A. Vasilevskaya, *Phys. Lett. B* **345**, 490 (1995).
- [92] R. Kitano, M. Koike, and Y. Okada, *Phys. Rev. D* **66**, 096002 (2002); **76**, 059902 (2007).
- [93] J. Barranco, D. Delepine, V. G. Macias, and L. Lopez-Lozano, [arXiv:1404.0454](https://arxiv.org/abs/1404.0454).
- [94] F. Wauters, A. Garca, and R. Hong, *Phys. Rev. C* **89**, 025501 (2014); **91**, 049904 (2015).
- [95] J. S. Hagelin, *Nucl. Phys.* **B193**, 123 (1981).
- [96] A. Dighe, A. Kundu, and S. Nandi, *Phys. Rev. D* **76**, 054005 (2007).
- [97] J. P. Leveille, *Nucl. Phys.* **B137**, 63 (1978).
- [98] G. Bhattacharyya, J. R. Ellis, and K. Sridhar, *Phys. Lett. B* **336**, 100 (1994); **338**, 522 (1994).
- [99] T. E. Chupp *et al.*, *Phys. Rev. C* **86**, 035505 (2012).
- [100] A. Kozela *et al.*, *Phys. Rev. Lett.* **102**, 172301 (2009).
- [101] R. Huber, J. Lang, S. Navert, J. Sromicki, K. Bodek, St. Kistryn, J. Zejma, O. Naviliat-Cuncic, E. Stephan, and W. Haeberli, *Phys. Rev. Lett.* **90**, 202301 (2003).
- [102] E. G. Adelberger, C. Ortiz, A. García, H. E. Swanson, M. Beck, O. Tengblad, M. J. G. Borge, I. Martel, H. Bichsel (the ISOLDE Collaboration), *Phys. Rev. Lett.* **83**, 1299 (1999); **83**, 3101 (1999).